RSC Advances

REVIEW

View Article Online
View Journal | View Issue

CrossMark click for updates

Cite this: *RSC Adv.*, 2015, **5**, 93002

New advances in non-fullerene acceptor based organic solar cells

Chuanlang Zhan,* Xinliang Zhang and Jiannian Yao*

Non-fullerene organic solar cells (NF-OSCs), in which an n-type organic molecule instead of a fullerene derivative is utilized as the electron-acceptor material, have recently emerged as a new topic in the field of organic solar cells. Replacement of the traditional fullerene acceptor in the photoactive layer of a normal organic solar cell with the organic acceptor gives rise to several advantages, like light absorption and energy level tunability, diversity of donor-to-acceptor combination, and large-scale production of acceptor materials. Studies on NF-OSCs can be traced back to 1986, when the first bilayered organic solar cell was proposed. Unfortunately, they has been advancing very slowly and the power-conversion-efficiency (PCE) was only approaching or exceeding 2% up to 2012. Fast advances have been driven forward since 2013, when the PCE value first broke through 4%, and the reported PCE value has now reached about 8% after a short period of 3 years. If we turn to natural systems such as the photosynthesis systems I and II, in which Nature utilizes organic molecules to accomplish high-efficiency solar-to-chemical energy conversion through the cascade unidirectional electron–hole transfer paths, we can rationally expect an even higher PCE and a convincing future for NF-OSCs. In this review, we will address recent new progress in this sub-branch of organic solar cells.

Received 1st September 2015
Accepted 1st October 2015

DOI: 10.1039/c5ra17715d

www.rsc.org/advances

Published on 08 2015. Downloaded on 06/08/2025 2:35:09 .

1. Introduction

Energy consumption supports the economic development of the world, and currently fossil energy sources such as natural gas, petroleum and coal are the major sources. For example, fossil energy sources were used for 82.1% of total energy consumption in the U.S. in 2013.[1] As we know, the reserves of fossil energy sources are limited and burning leads to the emission of CO_2 and other pollutant chemicals. Therefore, the development of clean and renewable energy sources has become one of the major scientific and technological topics of the 21st century and clean, green and sustainable solar energy is one of these sources. Currently, inorganic photovoltaic technology, such as silicon or cadmium telluride based technology,

Beijing National Laboratory of Molecular Science, CAS Key Laboratory of Photochemistry, Institute of Chemistry, Chinese Academy of Sciences, Beijing, 100190, P. R. China. E-mail: clzhan@iccas.ac.cn

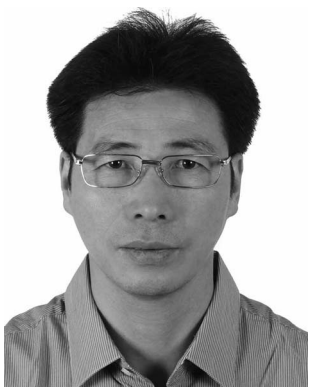

Chuanlang Zhan is a professor of chemistry at the Institute of Chemistry, Chinese Academy of Sciences (CAS). His research activities focus on synthesis and self-assembly of functional molecular materials, solar energy conversion and solar cells. He received a PhD degree (2000) in Organic Chemistry from the Institute of Photographic Chemistry, CAS, under the supervision of Prof. Duoyuan Wang, and joined the Institute of Chemistry, CAS, as a postdoctoral research fellow at CAS Key Laboratory of Organic Solids, Institute of Chemistry, CAS, and later was promoted to Associate Professor at this institute.

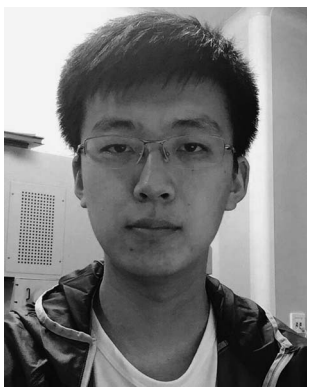

Xinliang Zhang received his BS degree from College of Chemistry and Molecular Engineering at Peking University in 2011. He is now a PhD student at the Institute of Chemistry, Chinese Academy of Sciences. His research interests include the synthesis and device engineering of organic solar cells.

This journal is © The Royal Society of Chemistry 2015

Published on 08 2015. Downloaded on 06/08/2025 2:35:09 .

holds the dominant position in industrial production, owing to its relatively mature technology and high power conversion efficiency (PCE) of over 20%.[2] Alternatively, organic photovoltaic cells utilize synthesis-accessible organic molecules as the light-capturing materials. They have several distinct advantages such as low-cost, mechanical flexibility, light weight, color-tunability, and semi-transparency. Particularly, the optoelectronic properties of organic materials can be easily tuned *via* organic synthesis to improve their solar photon capturing capability. The development of the bulk heterojunction (BHJ) structure[3] spans the gap between the short exciton diffusion length (typically, 5–20 nm) of organic semiconductors and the film thickness (typically 100 nm) required for efficiently capturing the solar photons. The solution-process technology endows bulk heterojunction organic solar cells (BHJ OSCs) with high potential for the mass production of flexible and cost-effective cells.

Since the first bilayered organic solar cell was proposed in 1986,[4] organic solar cells have been studied for over 30 years. Their efficiency has been increased from the initial 1% to the current 10–12% through donor-material and cell-structure innovations.[5,6] Recently, a new research topic has emerged in the field of organic solar cells: non-fullerene organic solar cells (NF-OSCs). Traditional OSCs utilize fullerene acceptors, typically [6,6]-phenyl-C_{61} (or C_{71})-butyric acid methyl ester ($PC_{61}BM$ or $PC_{71}BM$) as the electron-acceptor materials, while n-type organic molecules are selected to replace fullerenes as the acceptor materials in NF-OSCs. In the past 3 years, NF-OSCs have been paid increasing attention and fast advances have been achieved. Several review papers were published addressing small-molecule and polymeric organic acceptors before the end of 2013.[7–13] Several review papers have been recently published to address this research topic, typically from the molecular point of view.[14–16] In addition, this topic has been included in several recent review papers.[17–19] On the basis of the fast success in this newly emerging topic, we herein focus mainly on recent advances in the molecular design of organic acceptors, and, particularly, on the realization of efficient non-fullerene solar cells by addressing the donor-to-acceptor combinations, from the following three aspects: spectral coverage, energy level matching and film morphology.

Jiannian Yao received his PhD degree with Prof. Akira Fujishima at Tokyo University in 1993. Now he serves as a Professor of Chemistry at ICCAS, the president of the Chinese Chemical Society, and the vice president of the National Natural Science Foundation of China. His research interests are organic and inorganic optofunctional nanomaterials.

In this review article, we first introduce "Concept, classification and recombination mechanisms" (part 2), which includes the subparts of "What are NF-OSCs", "Why are NF-acceptors under consideration", "Classification of NF-OSCs", and "Recombination loss in a cell device" which is a key issue in developing an efficient NF-OSC as well as "Design principles for efficient organic acceptors". Then, we will go into the recent advances in both small-molecule (part 3) and polymer (part 4) acceptors and the challenges in designing high-efficiency NF-OSCs (part 5). The final part is about the conclusions and outlook (part 6).

2. Concept, classification and recombination mechanisms

2.1. What are NF-OSCs?

For a typical organic solar cell, the photoactive organic layer is sandwiched by a transparent and back electrode, respectively, forming a single-junction cell device. A single-junction cell device can be fabricated in either a conventional or an inverted configuration, depending on the flow direction of the mobile charge carriers (Fig. 1A). The free holes are collected by the transparent electrode and the mobile electrons are gathered by the back electrode in the convention-structured solar cell, while the holes and electrons are collected in an opposite manner in the inverted solar cell. Modification of the electrode surface by using an interlayer with an appropriate work function is necessary to form an Ohmic contact and energy level alignment between the inorganic electrode and the photoactive organic layer, allowing selective collection of the mobile charge carriers on the right electrode.[20,21] For example, the work function of PEDOT:PSS (poly(3,4-ethylenedioxythiophene):poly(styrenesulfonate)) is about 5.0 eV. Modification of the ITO surface with PEDOT:PSS can selectively allow the efficient transport of the mobile holes, down to the ITO electrode in a normal cell structure, while MoO_x is a commonly used hole transporting layer in an inverted configuration (Fig. 1B).

In BHJ OSCs, the photoactive layer comprises electron-donor (D) and electron-acceptor (A) materials, blended in a BHJ structure. The donor materials can be the polymer or small molecule and the acceptors can be the fullerene derivatives, *i.e.* $PC_{61}BM$ or $PC_{71}BM$ or n-type organic molecules. On the basis of the kind of acceptor material used in an OSC, either fullerene or organic, the resulting cell is called a fullerene or non-fullerene organic solar cell. For fullerene organic solar cells, the well-known polymer organic solar cells (PSCs) and small-molecule organic solar cells (SM-OSCs) are fabricated using polymers and small-molecules as the donor materials, respectively.

Thanks to community scientists' great efforts in the molecular design and synthesis of donor materials, either small-molecules or polymers, processing techniques for the optimization of organic blend film morphology, judicious interfacial engineering, and cell device structure, the PCE has been recently boosted to 10–11% for a single-junction state-of-the-art fullerene solar cell with small-molecules[24,25] or polymers[5,26–35] as the donor materials, and up to 11–12% for a tandem cell.[6,36,37]

Published on 08 2015. Downloaded on 06/08/2025 2:35:09 .

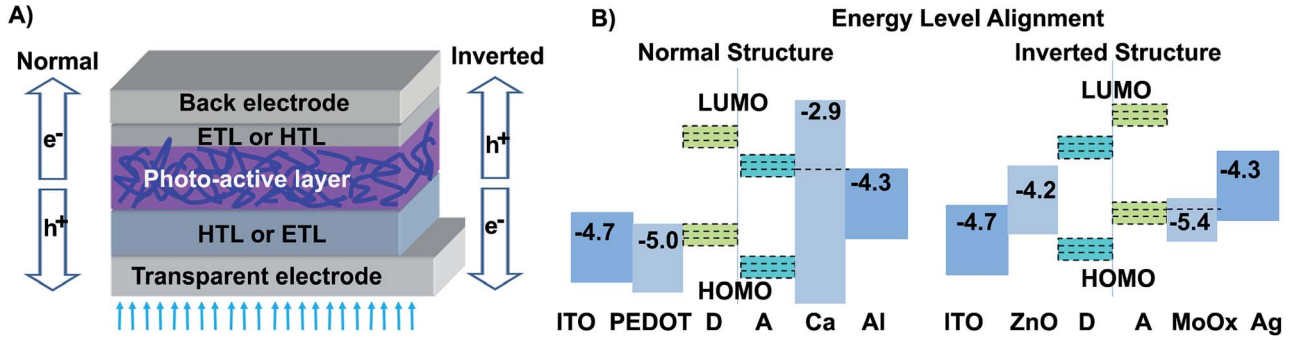

Fig. 1 (A) Depiction of a typical conventional and inverted device structure, in which a hole transporting layer (HTL) and an electron transporting layer (ETL) are selectively utilized to modify the transparent and back electrode, respectively, to allow the selective collection of the mobile holes and electrons. (B) Schematic models of energy level alignments in the conventional and inverted cell.

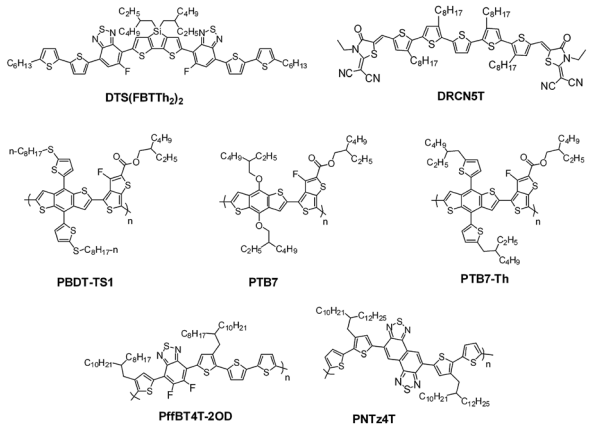

Fig. 2 The molecular structures of typical small-molecule and polymer donors from which a PCE of 10–11% or 11–12% has been realized for single-junction or tandem solar cells. The molecules are reported as follows: **PTB7** (E_g^{opt} = 1.63 eV),[22] **PTB7-Th** (1.58 eV),[23] **DTS(FBTTh$_2$)$_2$** (1.55 eV),[24] **DRCN5T** (1.60 eV),[25] **PBDT-TS1** (1.51 eV),[26] **PffBT4T-2OD** (1.55 eV),[5] and **PNTz4T** (1.54 eV).[34]

Fig. 2 presents typical polymer and small-molecule donors from which over 10% PCE has been realized.

With respect to the fullerene counterpart, the NF-OSC is slow over a long period of time. The reported PCE value went below or above 1% before 2010 (Fig. 3). The PCE value first broke through 2% at the end of 2010 by using a blend of a 2-dimensional (2D) conjugated polymer donor[38] and a perylene diimide (PDI) based polymer acceptor (with a PCE of 2.23%).[39] A year later, another value of 2.54% was published for a naphthalimide-vinyl-benzothiadiazole based small molecule acceptor blended with poly(3-hexylthiophene) (P3HT).[40] In 2013, the PCE value further broke through 4% by using a thienyl-bridged PDI dimer acceptor, so-called bis-PDI-T-EG, which was blended with the conjugated polymer of PBDTTT-C-T.[41] In this year, there were reported two kinds of PDI dimer acceptors, in which two PDI chromophores were covalently linked through their imide positions *via* a single bond[42] or through their bay positions *via* an aromatic unit.[43–45] The former gave a PCE of 3.2% when blended with PBDTTT-C-T.[42] The latter yielded a PCE of 0.3–2.5% when blended with P3HT, depending on the structure of the bridged aromatic unit[43,44] and the number of the substituent groups on the bay region of the PDI dimer.[45] Very recently, a PCE of close to 8% has been reported.[46] From Fig. 3, one can see that NF-OSCs have been advancing faster and faster since 2013 thanks to the great efforts of the community in acceptor material design, selection of the donor-to-acceptor system, optimization of the film morphology, as well as interlayer engineering between the organic photoactive layer and the electrode, as addressed in parts 3 and 4 of this paper. In short, NF-OSCs have emerged as a new, growing and interesting sub-branch in the field of organic solar cells in recent years.

2.2. Why are organic acceptors under consideration?

PCBM (including both $PC_{61}BM$ and $PC_{71}BM$ hereafter) is an excellent acceptor material, in particular, for utilization in organic solar cells. PCBM can not only finely intermix with donors to quench excitons but also forms nanoscale aggregate domains which, combined with its high electron affinity, benefits the acceptance of electrons from the donor semiconductor. Its spherical conjugated structure can not only greatly increase the chance of forming a beneficial alignment with the donor π-system in all directions for charge separation, but it also shows the capability of forming carrier-transport favourable nanoscale interpenetrating networks with the donor, which is helpful for charge transportation from the

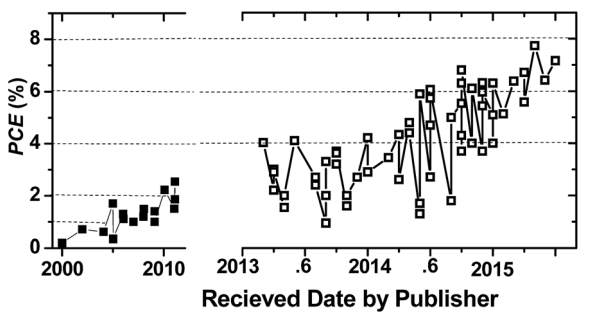

Fig. 3 A representative depiction showing the key historical PCE values achieved from solution-processed BHJ NF-OSCs *versus* the dates of the papers received by the publishers.

This journal is © The Royal Society of Chemistry 2015

Published on 08 2015. Downloaded on 06/08/2025 2:35:09 .

active layer to the electrode. Nevertheless, PCBM has several small drawbacks.[47] For example:

(1) There are no hydrogen atoms covalently linked to the fullerene backbone and an adduction reaction is the most frequently used way to chemically modify the fullerene backbone. Following this reaction, the energy level of the lowest unoccupied molecular orbital (LUMO) is raised by breaking down the conjugation of the π-electrons,[48] while it is difficult to establish conjugation between the π-electrons of the fullerene and those of the covalently attached functions, which limits the fine-tuning of its optoelectronic properties, shifting, for example, the absorption to the long wavelength range and further enhancing the absorptivity in the visible and near infrared (IR) region.

(2) The adduction reaction on the fullerene backbone is weakly selective and this not only lowers the yield of the target product but also magnifies the purification difficulty. Given that the impurity may be severely detrimental to the power conversion efficiency of PCBMs, specialist techniques, like high performance liquid chromatography (HPLC), are needed to produce high quality PCBMs,[49] which then elevates the PCBMs' price and limits the practical applications.

(3) As Fig. 4 displays, $PC_{61}BM$ has a very weak absorption beyond 425 nm in the solution state or beyond 545 nm in a thin-film, while $PC_{71}BM$ shows relatively stronger absorption in the visible region, typically before 750 nm. Therefore, the donor material in the fullerene solar cell plays an important role in absorbing the solar photons distributed in the visible and near infrared wavelength region. Thanks to the efforts of materials scientists, numerous donor materials have been successfully synthesized to harvest the solar photons at wavelengths longer than 500 nm. The absorption band position and shape, the bandgap or the absorption onset, and the LUMO/HOMO energy levels can be successfully fine-tuned with several synthetic strategies, such as the well-known and facile donor–acceptor (D–A) conjugation strategy and chemical modifications with polar heteroatoms, for example, for the synthesis of the high-efficiency small-molecule and polymer donor materials shown in Fig. 2. However, it is as yet a big challenge to synthesize a donor material that can absorb across a wide wavelength range, spanning, for example, 400 to 800 nm, and even up to 1000 nm, to capture solar photons as much as possible.

In striking contrast to fullerene acceptors, the chemical structure of non-fullerene organic acceptors can be more easily modified and their source materials are much more readily available. Their spectral coverage can be more easily tuned through chemical modification of the π-system. Therefore, the full coverage of the solar spectrum can become more easily attainable by judicious design of the acceptor molecules and then selection of an organic-donor-to-organic-acceptor combination, by combining, for example, a narrow bandgap donor material ($E_g < 1.6$ eV) with a medium bandgap acceptor material ($1.6 < E_g < 2.2$ eV), whose spectral coverage is complementary to that of the donor. For example, the PBDTTT-C-T:bis-PDI-T-EG system[41] whose absorption spectra are shown in Fig. 4. Meanwhile, tunability of the LUMO and HOMO energy levels of the organic acceptor can allow us to not only match the LUMO energy but also the HOMO energy between the organic donor and non-fullerene acceptor, which guarantees efficient charge separation for the excitons generated by the donor and acceptor phases, which dissociate through the so-called electron and hole transfer paths, respectively.[50]

As shown in Fig. 4a, the absorptivity of the $PC_{71}BM$ solution is above the order of 1×10^4 M^{-1} cm^{-1} in the visible region, typically from 400 to 550 nm. This absorption coefficient is comparable to most organic chromophores such as the well-known PDI.[19] Upon casting into a thin film, the absorbance of the $PC_{71}BM$ neat film is only slightly weaker, as the wavelength is beyond 500 nm, than that of a typical PDI dimer, bis-PDI-T-EG. From the blend films with PBDTTT-C-T as the donor material, for example, one can see that the PBDTTT-C-T film blended with bis-PDI-T-EG even has a relatively weaker absorption than the $PC_{71}BM$ blended film in the wavelength range before 500 nm, although a comparable absorption can be

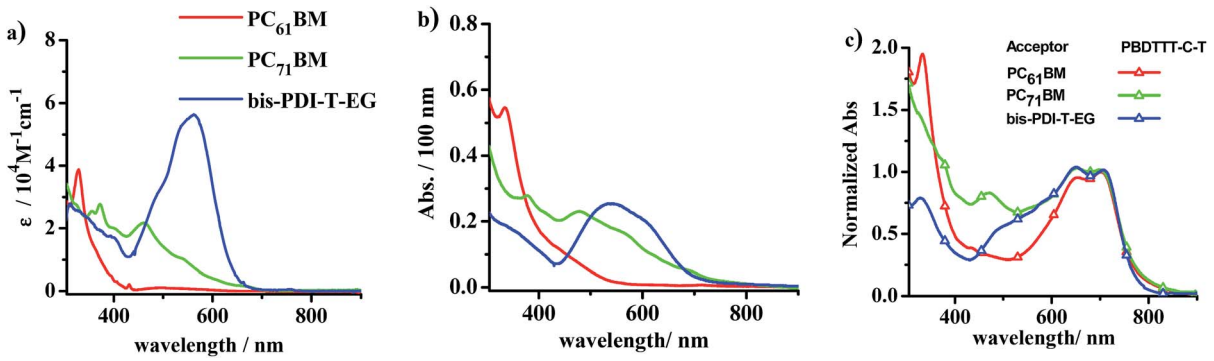

Fig. 4 The absorption spectra of $PC_{61}BM$ (red), $PC_{71}BM$ (green) and bis-PDI-T-EG (blue) in (a) chloroform (obtained with a concentration of 1×10^{-5} M) and (b) pristine films (spun-cast from the corresponding chloroform solution). (c) The absorption spectra of PBDTTT-C-T:$PC_{61}BM$ (red + triangles), PBDTTT-C-T:$PC_{71}BM$ (green + triangles), PBDTTT-C-T:bis-PDI-T-EG (blue + triangles) blended films (1 : 1, wt/wt). The PBDTTT-CT:$PC_{61}BM$ and PBDTTT-CT:$PC_{71}BM$ blended films were spun-cast from the corresponding *o*-dichlorobenzene (*o*-DCB) solution with 1,8-diiodooctane (DIO, 3% v/v). The PBDTTT-CT:bis-PDI-T-EG blended films were spun-cast from *o*-dichlorobenzene (*o*-DCB) solution with DIO (2% v/v) and treated by solvent vapour annealing as shown in the reported literature.[50] Each spectrum was obtained by averaging the data of five parallel experiments. The spectra in (c) are normalized to see the contribution of the acceptor materials to the absorption of the blend film.

Published on 08 2015. Downloaded on 06/08/2025 2:35:09 .

seen when the wavelength of the incident light is beyond 500 nm. Therefore, only the $PC_{61}BM$ blend film may have weaker absorption than organic acceptor blend, while the $PC_{71}BM$ blend normally absorbs the visible and near infrared solar photons in strength comparable to the organic acceptor blend with the same donor material.

Why are we interested in replacing the currently dominant and efficient fullerene acceptor with the n-type organic molecule? The reasons are related to, but not limited to, the above-mentioned drawbacks of PCBM over organic acceptors. Indeed, if we look to Nature, we can see that the natural photosynthetic systems I and II do utilize organic molecules to accomplish high-efficiency solar to chemical energy conversion, in which the photoinduced excitons can be efficiently separated and exploited with an internal quantum efficiency of nearly 100% through the cascade unidirectional electron–hole transfer paths. Accordingly, we reasonably believe that replacement of the fullerene acceptors with organic molecules should make sense. The big issue is which organic molecule can achieve high efficiency and how to realize it.

2.3. Classification of organic acceptors and NF-OSCs

Like donor materials, of which there are polymer and small-molecule types, organic acceptor materials can also be classified into small-molecule and polymer types. There are therefore four possible donor-to-acceptor combinations, from polymer donor and acceptor as well as small-molecule donor and acceptor, giving rise to four kinds of NF-OSCs, as Fig. 5 shows. Small-molecule acceptors have identical molecular structures and molecular weights, and high purity as well as batch-to-batch reproducibility. They are commonly synthesized from photoactive π-aromatics by stepwise coupling procedures. In contrast, polymer acceptors are normally synthesized by polymerization from photoactive π-aromatics and there is generally a distribution of molecular weight, as deduced from the weight-average molecular weight (M_w), number-average molecular weight (M_n), and polydispersity index (PDI). Studies have pointed out that different molecular weight distributions should lead to different cell performances.[51] Therefore, the batch-to-batch difference in the cell performance of polymer-based solar cells is normally significant.

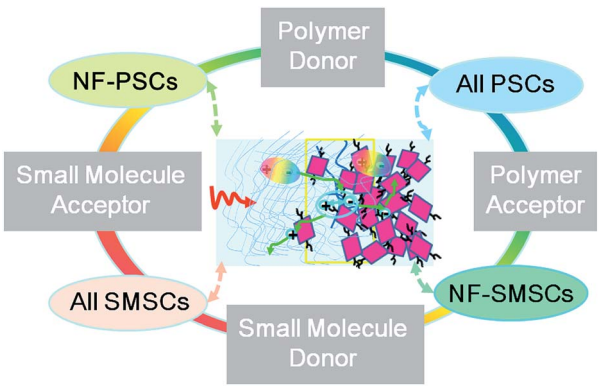

Fig. 5 Four possible organic-donor-to-organic-acceptor combinations arising for non-fullerene solar cells: the combination of polymer donor to polymer acceptor gives rise to the so-called all polymer organic solar cells (all PSCs);[52] the combination of small-molecule donor to small-molecule acceptor gives rise to the so-called all small-molecule organic solar cells (all SMSCs).[47,53] Herein, we named the polymer donor to small-molecule acceptor and the small-molecule donor to polymer acceptor systems non-fullerene polymer organic solar cells (NF-PSCs) and non-fullerene small-molecule organic solar cells (NF-SMSCs), simply following the classifications of the fullerene based organic solar cells; *i.e.* polymer organic solar cells (PSCs) and small-molecule organic solar cells (SMSCs), respectively.

2.4. Recombination loss in OSCs

The PCE (%) of a solar cell device is defined by the equation $PCE = J_{sc}V_{oc}FF/P_{in}$, wherein J_{sc} is the short-circuit current-density in mA cm^{-2}, V_{oc} is the open-circuit voltage in V, FF is the fill-factor in %, and P_{in} is the incident light intensity in mW cm^{-2}. Under the standard illumination conditions, the incident light intensity is 100 mW cm^{-2}, which can be provided by an AAA-grade simulated AM 1.5G light source. The cell parameters of J_{sc}, V_{oc}, and FF are derived from the experimental current-density–voltage (J–V) curve (Fig. 6). The FF is the graphic measurement from the J–V curve and is defined as $FF = (V_{mpp}J_{mpp})/(V_{oc}J_{sc})$, where V_{mpp} and J_{mpp} are the J and V values at the maximum power point (mpp).

Today, the efficiency of NF-OSCs lags behind their fullerene counterparts. Because the LUMO energy level of organic acceptors can be tuned towards a higher-lying level than that of PCBMs, the V_{oc} is normally higher than PCBM based solar cells when blended with the same donor material and using an identical cell structure. The lower efficiency is usually derived from the lower J_{sc} and FF, both of which are deeply related to the recombination loss and carrier mobility and lifetime. We herein paid attention to the recombination loss in a solar cell device.

The experimental current (J), as shown in the J–V characteristic curve, can be expressed by the formula $J = ne\mu E$, where n is the photogenerated carrier concentration, e is the electric charge, μ is the carrier mobility and E is the electric field. The mobile carrier's concentration and mobility are two experimental factors that we can manipulate through material design and film morphology control.

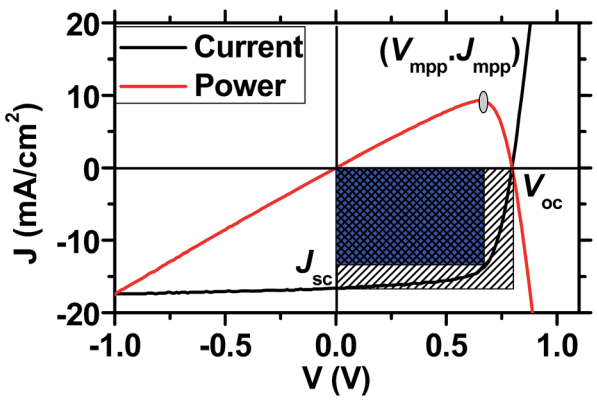

Fig. 6 Typical current-density–voltage (J–V) characteristics (black) and the relative output electric power–voltage curve (red) from a BHJ solar cell under illumination by an AAA-grade AM1.5G simulator.

This journal is © The Royal Society of Chemistry 2015

Published on 08 2015. Downloaded on 06/08/2025 2:35:09 .

The mobile carriers are initially generated at the donor-to-acceptor interfaces and transport, respectively, through the interpenetrating acceptor and donor phases. Then they are collected by the right electrode. The ultimate concentration of the mobile carriers by the right electrode, n, is defined by exciton generation and recombination losses, and can be written as $n = n_0 - an_0$, where n_0 is the total concentration of the excitons generated by both the blended donor and acceptor phases, a is a dimensionless parameter, as defined by $a = (n_0 - n)/n_0$, representing the recombination loss during the exciton diffusion and separation as well as mobile carrier drift and collection. Normally $a \leq 1$. This is because recombination loss always exists in organic semiconductor films.

The recombination mechanisms in a BHJ solar cell device involve both the so-called geminate and non-geminate recombination losses. In the photoactive layer of a BHJ OSC device, the blended donor and acceptor materials can both absorb solar photons and generate excitons, the singlet excitons (Fig. 7A). The excitons' concentration is dependent on the light-capturing ability of the photoactive layer. The excitons can be relaxed down to the ground state *via* both the radiative and nonradiative paths before they get to the donor-to-acceptor interface.

After accessing the donor-to-acceptor interface, the excitons are separated *via* the electron and hole transfer paths (Fig. 7B), respectively, forming mobile carriers, *i.e.* free electrons and holes. Current studies demonstrate that there exists an intermediate charge-transfer (CT) state associated with the exciton dissociation. For example, after the excited electron goes from the lowest unoccupied molecular orbital (LUMO) of the donor to that of the acceptor, the electron and hole are both bound together strongly by their mutual Coulombic force, forming a CT state.[54] The bound electron–hole pairs are then spatially dissociated, driven by the internal field (V_{int}), forming free electrons and holes, *i.e.* free charge carriers.[55] The V_{int} is defined by the equation $V_{int} = V_{bi} - V_{app}$. Here V_{bi} is the build-in voltage defined as J_{ph} is zero and V_{app} is the applied bias. Other than the separation, the bound electron–hole pairs can be recombined to go back to the ground state (Fig. 7B).

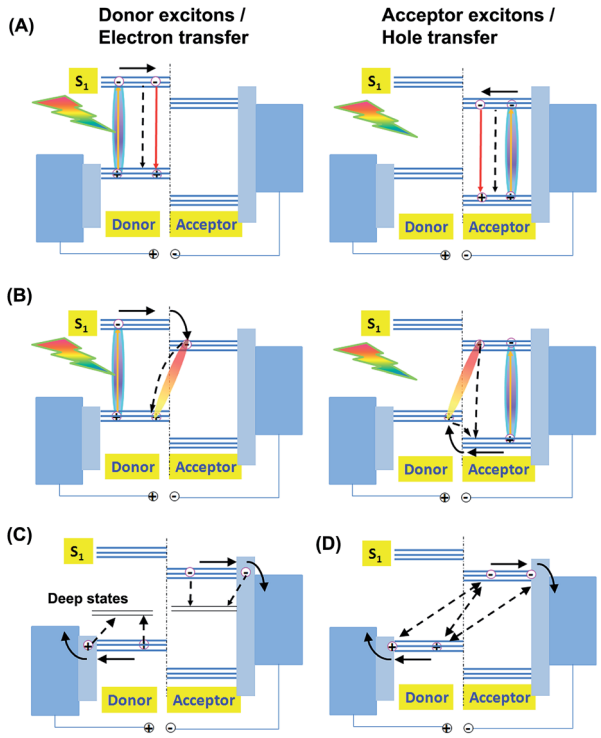

Fig. 7 Schematic depictions of the generation of donor excitons and acceptor excitons, electron and hole transfer, and loss mechanisms *via* exciton decay (A), recombination of bound electron–hole pairs (B), and recombination of mobile electrons and holes as trapped by deep states (C) or in a bimolecular mechanism (D).

The free electrons and holes, respectively, drift across the acceptor and donor phases, driven by the internal field, and are swept out down to the right electrode and then collected. Accompanying the carrier transportation and collection, the free carriers can be captured by traps (band tails) (Fig. 7C) or recombined between the mobile electron and hole pairs (Fig. 7D).

Taken together, the factor a is a product of the losses from exciton decay, recombination at the donor-to-acceptor interfaces and that from carrier transportation and collection. Nonradiative decay is an important way of inducing exciton loss before they move to the donor-to-acceptor interface (Fig. 7A). The effective exciton diffusion length is usually short, typically 5–20 nm, in organic semiconductor films and control of the phase size so that it is comparable to the exciton diffusion length is a prerequisite for realization of efficient BHJ OSCs. The exciton loss restricts the maximum generation rate of the obtainable bound electron–hole pairs (G_{max}^{e-h}, in $m^3\ s^{-1}$)[56,57] in a given cell device. The relationship between the G_{max}^{e-h} and the maximum generation rate of the excitons ($G_{max}^{exciton}$, in $m^3\ s^{-1}$) can be presented by an exciton loss factor of a_1 according to $G_{max}^{e-h} = (1 - a_1)G_{max}^{exciton}$. The G_{max}^{e-h} is defined by the formula $G_{max}^{e-h} = J_{ph,sat}/eL$,[56,57] where L is the thickness of the active layer and $J_{ph,sat}$ is the reverse saturated photocurrent, J_{ph}, which is related to the experimental light current J_L and the dark diode current J_D on the basis of $J_{ph} = J_L - J_D$. In a state-of-the-art cell device, the phase size follows the length range of the effective exciton diffusion length and the exciton loss factor of a_1 can be assumed to be close to one.

The recombination losses of the bound electron–hole pairs and the free electrons and holes include so-called monomolecular and bimolecular loss mechanisms. The monomolecular one refers to any first-order processes, involving the geminate losses of the bound electron–hole pairs, *i.e.* the CT states recombine before the bound electron–hole pairs separate (Fig. 7B), and the Shockley–Read–Hall (SRH) recombination induced by the deep states at the donor-to-acceptor interfaces, organic domain-to-domain interfaces and active layer-to-electrode interfaces and in the donor/acceptor domain phases (Fig. 7C). The geminate loss can be reflected by using femtosecond (fs) transient absorption pump-probe experiments.[58] The bimolecular one is a second-order process, referring to the recombination of free electrons and holes (Fig. 7D). If we use a_2, a_3 and a_4 to describe the loss following the geminate recombination of the CT states, SRH recombination and bimolecular mechanism of free electrons and holes, respectively, the total

Published on 08 2015. Downloaded on 06/08/2025 2:35:09 .

loss can be written as $a = a_1a_2a_3a_4$. However, it is as yet difficult to quantify these loss factors.

The recombination losses of the free electrons and holes can be qualitatively reflected by the incident light power dependent *J–V* characteristics, which are measured from a given cell device by varying the incident light power (P_0). For example, from one sun down to 0.01 sun. At short-circuit where the V_{int} is large enough to efficiently sweep out the photogenerated free electrons and holes prior to recombination, the loss is dominated by the SRH recombination. This mechanism can be described using $J_{sc} \propto P_0^{\alpha}$.[59] If all of the free electrons and holes can be collected under the short-circuit conditions, meaning the bimolecular loss is negligible, the J_{sc} should be linearly dependent on the incident light power with $\alpha = 1$. When the fitting α value is smaller than one it suggests contribution from the bimolecular mechanism, and a smaller α value means that a more serious bimolecular loss is involved. At open-circuit the photogenerated free electrons and holes all recombine. The recombination mechanism can be reflected by the formula $V_{oc} \propto nkT/q \ln(P)$,[60] where k, T and q are the Boltzmann constant, the temperature in Kelvin and the elementary charge, respectively. Principally, if the bimolecular process dominates the recombination, the fitting n value should be one. As the SRH mechanism is involved, the recombination from shallow traps competes with the bimolecular and the fitting n value deviates from one: A larger n value indicates a more serious loss is involved for the SRH recombination.

In addition to manipulating the recombination loss by optimization of the film morphology and modifications of the electrode surface, enhancement of the light-capturing ability of the photoactive donor and acceptor materials can increase the maximum generation rate of the excitons. Hence, synthesizing donor and acceptor materials with a higher absorptivity, a wider solar spectrum coverage, and a lower bandgap is another goal, besides the reduction of the recombination loss, of materials scientists towards improving the current-density (Fig. 8A).

The energy offset between the LUMOs of the donor and acceptor materials ($\Delta E_{LUMO} = E_{LUMO,donor} - E_{LUMO,acceptor}$), and that between the highest occupied molecular orbitals (HOMOs) of the donor and acceptor materials ($\Delta E_{HOMO} = E_{HOMO,donor} - E_{HOMO,acceptor}$) are the driving forces for the singlet excitons to overcome their mutual Coulombic binding energy, driving the excited electron transfer from donor to acceptor and the hole transfer from acceptor to donor, respectively. It is normally accepted that the LUMO energy level of the donor should be at least 0.3 eV higher than that of the acceptor for efficiently driving the separation of the singlet donor excitons. The V_{oc} is widely observed to correlate with the energy level difference between the donor HOMO and the acceptor LUMO, as defined by $E_{DA} = E_{LUMO,acceptor} - E_{HOMO,donor}$. Upon photoexcitation, a CT state is formed at the donor-to-acceptor interface. A shift of the energy level of the CT state will lead to a change of V_{oc}.[61] Electronic coupling[62] and composition[63] between the donor and acceptor materials, and energy ordering[64] are other factors that influence the V_{oc} value. Since the energy level of the frontier molecular orbitals, *i.e.* the LUMO and HOMO, determine the material's bandgap, judiciously engineering the energy levels of the frontier molecular orbitals and the absorption spectrum are both the most important issues, while it is as yet a big challenge to meet the criteria required for the synthesis of efficient donor–acceptor materials, *i.e.* simultaneously guaranteeing a narrow bandgap, an appropriate driving force for efficient exciton-separation, and a high V_{oc}.

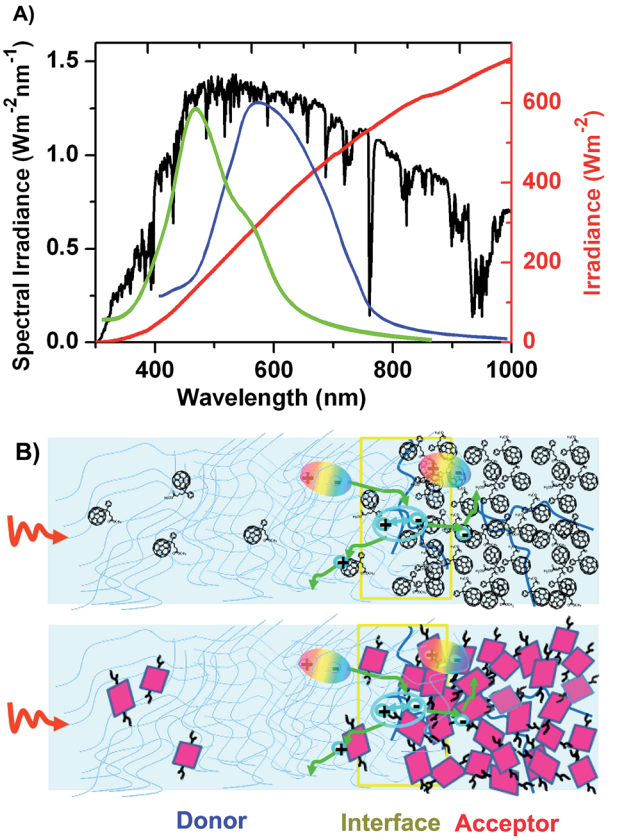

Fig. 8 (A) The solar spectrum (black), integrated irradiance *versus* wavelength (red) and modelling absorption spectra (green and blue) of donor–acceptor materials. (B) Schematic depiction of phase-separated donor and acceptor rich phases and their interface. The acceptor molecules are shown by the spherical PCBM molecules (upper) or by planar rectangles representing organic molecules (lower), respectively.

With respect to the understanding of J_{sc} and V_{oc}, we have learned much less on FF as yet. The recombination loss significantly scales the FF value. As the bimolecular loss is reduced, the *J–V* curve will become steep near the open-circuit condition, and as the monomolecular loss becomes weak, the curve near the short-circuit condition will be flat. Generally, a higher FF value may be achieved through reduction of the recombination loss by optimizing the film morphology of the active layer, modification of the electrode-active layer interface, and an increase of the carrier mobility and lifetime. Nevertheless, achieving a high FF value is as yet a big challenge for NF-OSCs.

2.5. Design principles for efficient organic acceptors

Similar to the requirements for efficient donor materials, a proper efficient organic acceptor should meet the following

 This journal is © The Royal Society of Chemistry 2015

Published on 08 2015. Downloaded on 06/08/2025 2:35:09 .

prerequisites: solar photon capturing ability, electron affinity and mobility, and self-assembling and phase-separation ability related to the formation of nanoscale interpenetrating networks with the blended donor material.

The photoactive layer consists of the blended donor and acceptor materials. Absorptivity of an organic material determines how many solar photons at a given wavelength can be absorbed, and its absorption band shape and bandgap determines the wavelength region within which the solar photons can be captured. As we know, upon photoexcitation an organic molecule normally gives an absorption band in a certain wavelength region with an absorption peak and a high and low energy edge, respectively, as demonstrated by the well-known Jablonski diagram. Accordingly, one facile way to cover the solar spectrum as widely as possible is to complement the absorption spectra of the donor and acceptor. For example, the donor is arranged to absorb low energy solar photons, while the acceptor is arranged to absorb high energy photons. This requires that we must comprehensively consider the absorptivity, bandgap and energy levels of the frontier molecular orbitals to meet the requirements of light absorption and electron affinity when designing acceptor molecules.

Other than the absorption property and the energy levels, film morphology is another key factor, because efficient charge generation and transportation are both limited by the formation of an ideal film morphology, including the formation of nanoscale interpenetrating networks, which are beneficial for exciton-separation, and long-range backbone-to-backbone packing, which is helpful for mobile carrier transport to the right electrode. Organic acceptors comprise planar aromatic π-units. This character is distinctly different to the spherical shape of the fullerene π-system. It is to date a big challenge to achieve both nanoscale interpenetrating networks and long-range molecular ordering from an organic acceptor and an organic donor system. Besides this, the donor-to-acceptor interfacial structure (Fig. 8B) plays an important role in the charge separation,[65–68] and hence, special considerations should be taken into account when designing organic acceptor molecules.

The fast development of modern physical and organic chemistry provides us the possibility to "design" the absorption band position and frontier molecular orbitals; for example, by carefully selecting and engineering the conjugation size of aromatic π-systems and electron-donating or accepting substituent groups on the π-systems. The rich means for carbon–carbon bond formation, as built by modern organic synthetic chemistry, for example the well-known and facile Stille and Suzuki coupling reactions, allows us to accomplish the synthesis of the designed organic molecules. With respect to knowledge of the optoelectronic properties of an organic molecule, the understanding of the molecular assembly is relatively poor and we cannot "predict" the aggregation behavior of an organic molecule and the underlying structure of the assembled aggregates. Moreover, we have not yet developed the powerful tools needed to "see" the intrinsic underlying structure of organic aggregates. Therefore, designing the film morphology is much more difficult than the prediction of the optoelectronic properties of an organic molecule system.

3. Small-molecule non-fullerene acceptors

3.1. PDI based small molecules

PDI is a traditional n-type semiconducting dye chromophore. Its absorption appears around 500 nm as a band in between 400 and 600 nm. Its absorptivity is in the order of 10^4 to 10^5 M^{-1} cm^{-1}. Its LUMO energy is around −4 eV and its electron mobility can be over 1 cm^2 V^{-1} s^{-1}.[69] Additionally, PDIs are stable to light, heat, and chemicals.[19,70] These optoelectronic properties make PDI units a potential candidate for constructing organic acceptors. However, molecular self-assembly studies on PDI derivatives have clearly demonstrated that the large planar π-system of the PDI chromophore always leads to the formation of hundreds of crystalline aggregates.[19,70–72] Accordingly, strong self-trapping of the excitons takes place within the large aggregates, which severely limits the exciton diffusion/separation efficiencies and further decreases the PCEs of the cell devices.[73] So far, several chemical modification approaches have been approved as facile ways to reduce the aggregation tendency for PDI chromophores (*vide post*). These approaches normally proceed at the nitrogen position, on the bay region (1, 6, 7 and 12-positions), or even on the 2, 5, 8 and 11-positions (headland positions) (Fig. 9A), including imidization using soluble side chains and/or aromatic moieties, or even the formation of twisted dimeric, trimeric and tetrameric conjugation backbones.

PDI monomer. The oldest strategy to synthesize soluble PDI derivatives is to introduce soluble alkyl chains on the nitrogen positions. One of the well-known PDI acceptors is the derivative

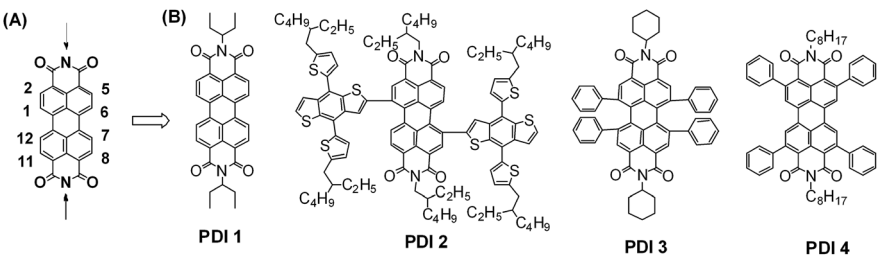

Fig. 9 (A) Available chemical modification positions on the PDI core and (B) chemical structures of typical PDI monomer based small-molecule acceptors.

Published on 08 2015. Downloaded on 06/08/2025 2:35:09 .

whose nitrogen positions are functionalized with the 1-ethylpropyl group, giving **PDI 1** (Fig. 9). This PDI acceptor normally had a PCE of <1% when blended with donor materials.[19] A recent case was reported by Bazan and coworkers, in which **PDI 1** was blended with the low bandgap small-molecule donor of (*p*-DTS(FBTTh$_2$)$_2$) in a 1 : 1 weight ratio, which gives a PCE of 3%.[74] Zhan and coworkers revealed that a higher donor-to-acceptor weight ratio of 1.3 : 1 can improve the donor-to-acceptor compatibility and formation of smaller phase domains (20 *vs.* 40 nm), which led to more efficient quenching of the donor and acceptor fluorescent emission, generating a higher G_{max}^{e-h} value. As a result, a higher J_{sc}, a higher FF and a higher PCE of 5.1% were achieved (Table 1). The good correlation between the acceptor phase size and the experimental J_{sc} value indicates that the morphology of the acceptor domain plays an important role.[75] Using the conjugated polymer of PBDTTT-C-T[76] as the blended donor material with 70% **PDI 1** (wt%), Keivanidis and coworkers demonstrated a PCE of 3.7% through the use of 0.4% 1.8-diiodooctane (DIO) as the solvent additive.[77] Further investigations on the local structural order and molecular packing indicated that electronic connectivity between the large domains of **PDI 1** reduced the electron mobility and the local disorder of the PDI domains was essential for efficient electron transport.[78,79] From transient absorption pump-probe spectroscopy, Laquai and coworkers illustrated that the charge separation between **PDI 1** and PBDTTT-C is strongly field-dependent. Upon excitation, both the PDI and polymer excitons undergo fast charge transfer on a time scale of several tens of picoseconds. However, the photoinduced electron transfer efficiency is only half of that in a polymer:fullerene blend, and a significant fraction of the charges generated at the interfaces from the PDI excitons are lost due to geminate recombination, both of which contribute to the low FF and J_{sc}. The authors speculated that only about 25% of the initial photoexcitations generates free charges.[80] In contrast, Durrant and coworkers demonstrated that both charge separation and recombination dynamics from PDI:PBDTTT-C-T blend are remarkably similar to those from the PC$_{71}$BM:PBDTTT-C-T system and they suggested that slower charge transport and stronger non-geminate recombination loss during charge collection are responsible for the inferior performance of the PDI based blend.[81] In any case, recombination loss is likely a major role in an NF-OSC device, with respect to the fullerene solar cell.

The LUMO and HOMO energy levels of **PDI 1** are −3.82 and −5.87 eV, respectively.[75] With the two aromatics of 4,8-bis(2-(2-ethylhexyl)thienyl)benzo[1,2-*b*:4,5-*b*′]dithiophene (2T-BDT) covalently conjugated onto the 1 and 7 positions of the PDI core, Zhan, Yao and coworkers reported a narrow bandgap acceptor molecule, **PDI 2**, with an optical bandgap of 1.6 eV. Its LUMO energy was reduced down to −3.95 eV, while the HOMO energy was raised to −5.57 eV. The steric effects between the BDT and PDI planes led to the formation of a twisted conformation, improving the solution-processability. When blended with the commercial poly(3-hexylthiophene) (P3HT), a PCE of 1.7% was obtained.[82] Sun and coworkers recently reported that the neat film of 1,6,7,12-tetraphenyl substituted **PDI 3** had an absorption spectrum very similar to that in solution because the aggregation tendency was significantly suppressed by the introduction of the cyclohexyl side-chains and the formation of a twisted conformation between the phenyl group and the PDI core. **PDI 3** gave a PCE of 4% after it was blended with the efficient polymer donor of PTB7-Th and the use of 1% chloronaphthalene (CN) as the solvent additive.[83] By introducing four phenyl groups at the 2, 5, 8 and 12-positions, Marks, Wasielewski and coworkers demonstrated that this different molecular strategy can promote the formation of slip-stacking of the PDI π-systems, which prevents the coupling necessary for rapid excimer formation. The resultant acceptor, **PDI 4**, was blended with the donor polymer PBTI3T, yielding a PCE of 3.7% with a top V_{oc} of 1.0 V.[84]

PDI dimer. Construction of a dimeric PDI backbone is an alternative approach towards a twisted conformation, and hence, reduction of aggregation tendency, affording solution-processable PDI acceptors. The first reported example was **PDI 5** (Fig. 10), in which two PDI units were linked through a single N–N bond. Narayan and coworkers illustrated that the use of PBDTTT-C-T as the blend donor material afforded a PCE of around 3% (Table 2).[85] A further study indicated that both polymer and PDI excitons underwent fast dissociation with similar time scales of a few picoseconds at the donor–acceptor interface.[42] A recent study by Wang, Hou and coworkers indicated that the replacement of C_7H_{15} with C_5H_{11} in **PDI 5** and blending with another high-efficiency donor polymer of PBDT-TS1 gave an improved PCE of 5.58% with an increasing J_{sc}, V_{oc} and even FF with an inverted cell structure.[86] When the polymer

Table 1 Optoelectronic properties, electron–hole mobilities, and cell parameters from PDI 1–4

PDI	Donor	E_g^{opt}[a] (eV)	LUMO/HOMO (eV)	μ_e/μ_h ($\times 10^{-3}$ cm^2 V^{-1} s^{-1})	J_{sc} (mA cm^{-2})	V_{oc} (V)	FF (%)	PCE[b] (%)	Ref.
1	DTS(FBTTh$_2$)$_2$	—/1.55		0.17/0.07	7.4	0.78	52	3.0	74
1	DTS(FBTTh$_2$)$_2$	1.91/1.55	−3.82/−5.87	4.5/1610	9.84 ± 0.20	0.80 ± 0.00	64.1 ± 0.5	5.07 ± 0.10	75
1	PBDTTT-C-T	—/1.58		0.006/0.08	8.10 ± 0.06	0.80 ± 0.01	51.9 ± 0.7	3.64 ± 0.10	76
2	P3HT	1.63/2.0	−3.95/−5.57	0.02/—	5.3	0.61	51	1.66	82
3	PTB7-Th	1.85[c]/1.58	−3.82/−5.69	—	10.1	0.87	46	4.1	83
4	PBTI3T	2.01/1.75[c]	−4.01/−6.02	2.4/—	6.6	1.0	55	3.67	84

[a] Optical bandgap obtained from the neat A and D film and presented in the manner of A/D. [b] Under illumination with AM 1.5G, 100 mW cm^{-2}. [c] Calculated from the absorption edge (λ_{edge}^{abs}) with the equation of $E_g^{opt} = 1240/\lambda_{edge}^{abs}$ (eV). The value of λ_{edge}^{abs} was obtained from the absorption spectrum presented in this reference.

 This journal is © The Royal Society of Chemistry 2015

Published on 08 2015. Downloaded on 06/08/2025 2:35:09 .

PTB7-Th was selected to be blended with **PDI 5b**, a similar PCE of 6.41% was achieved.[87]

Linkage of two PDI units through the bay region is another dimeric way towards twisted, solution-processable PDI dimer acceptors. Zhan, Yao and coworkers reported a series of PDI dimers, **PDI 6–8** for example. Using a thienyl unit as the aromatic linker, the LUMO and HOMO energy levels of the resultant PDI dimer were raised from −3.95/−5.83 eV for **PDI 6a** to −3.84/−5.65 eV for **PDI 6b** and −3.84/−5.57 eV for **PDI 7** after 2 and 4 electron-donating alkoxyl side-chains were introduced on the bay region, respectively, and **PDI 7** showed the best compatibility with P3HT, leading to the best PCE of

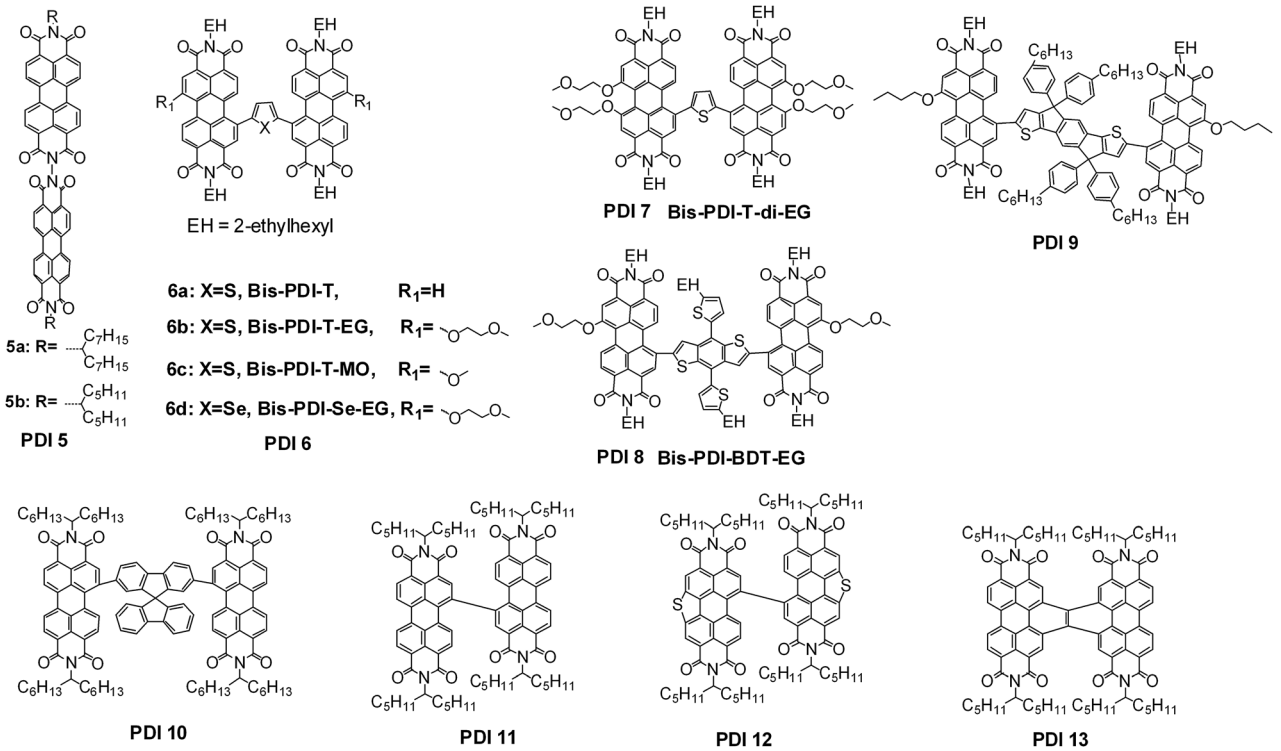

Fig. 10 Chemical structures of several typical PDI dimer acceptors.

Table 2 Optoelectronic properties, electron–hole mobilities, and cell parameters from PDI 5–13

PDI	Donor	$E_g^{opt a}$ (eV)	LUMO/HOMO (eV)	μ_e/μ_h ($\times 10^{-3}$ cm^2 V^{-1} s^{-1})	J_{sc} (mA cm^{-2})	V_{oc} (V)	FF (%)	PCE^b (%)	Ref.
5a	PBDTTT-C-T	—/1.58	−4.06/−6.02	0.15/0.27	9	0.77	0.46	3.2	42
5b	PBDT-TS1	2.04/1.51	−4.06/−6.02	1.2/8.9	12.85 ± 0.23	0.80 ± 0.01	53 ± 2	5.45 ± 0.12	86
5b	PTB7-Th	—/1.58	−4.06/−6.02	1.2/8.9	13.12 ± 0.33	0.79 ± 0.00	60 ± 1	6.41	87
6a	*p*-DTS(FBTTh$_2$)$_2$	1.82/1.55	−3.95/−5.83	0.46/230	7.31 ± 0.23	0.73 ± 0.00	65.3 ± 2.2	3.47 ± 0.13	90
6b	PBDTTT-C-T	1.76/1.58	−3.84/−5.65	6.1/10.3	12.54 ± 0.17	0.84 ± 0.01	56.67 ± 2.	6.00 ± 0.06	91
6b	BDT-T-DPP	1.76/1.64	−3.84/−5.65	16/22	4.66	0.92	47	2.01	47
6c	PBDTTT-C-T	1.76/1.58	−3.84/−5.65	1.2/5.6	9.99 ± 0.18	0.78 ± 0.01	52.8 ± 2.0	4.22 ± 0.12	92
6d	PBDTTT-C-T	1.75/1.58	−3.84/−5.61	4.7/9.3	10.60	0.79	47.93	4.01	89
7	P3HT	1.76/2.0	−3.84/−5.57	0.71/230	3.83	0.67	60.0	1.54	45
8	P3HT	1.81/2.0	−3.84/−5.48	0.34/77	5.83	0.68	49	1.85	44
9	BDT-T-DPP	1.54/1.64	−3.83/−5.53	0.0023/0.020	7.75	0.95	42	3.12	93
10	P3HT	2.0^c/2.0	−3.71/−5.71	0.071/—	5.92	0.61	65	2.35	43
10	PffBT4T-2DT	2.0/1.55	−3.83/−5.90	0.18/2.3	10.7 ± 0.4	0.98 ± 0.01	57 ± 1	6.0 ± 0.3	95
11	PBDTTT-C-T	2.1/1.58	—	—	10.58	0.73	46.8	3.63	96
11	PBDTBDD	2.1/1.77^c	−3.87/−5.95	—/1.0	8.26	0.87	61.1	4.39	97
11	PTB7-Th	2.1/1.58	−4.04/−6.13	0.033/43.6	11.98 ± 0.34	0.80 ± 0 0.01	59 ± 1	5.90	100
12	PDBT-T1	2.20/1.85	−3.85/—	2.8/1.2	11.65 ± 0.21	0.90 ± 0.003	65.5 ± 0.58	6.90 ± 0.15	101
13	PTB7-Th	2.1/1.58	−3.77/−6.04	0.34/0.29	13.5 ± 0.2	0.796 ± 0.005	55 ± 1	5.94 ± 0.07	102

[a] Optical bandgap obtained from the neat A and D film and presented in the manner of A/D. [b] Under illumination with AM 1.5G, 100 mW cm^{-2}. [c] Calculated from the absorption edge (λ_{edge}^{abs}) with the equation of $E_g^{opt} = 1240/\lambda_{edge}^{abs}$ (eV). The value of λ_{edge}^{abs} was obtained from the absorption spectrum presented in this reference.

Published on 08 2015. Downloaded on 06/08/2025 2:35:09 .

1.54% of the three dimers.[45] The HOMO could be further increased to −5.48 eV when the electron-donating 2T-BDT was selected as the aromatic π-bridge, giving **PDI 8**, which had a PCE of 1.9% when using P3HT as the donor polymer. It was hypothesized that the highly twisted conformation can provide so-called steric-pairing effects for the self-organization of the twisted PDI dimer molecules.[44] The PDI dimer's LUMO energy can be fixed at −3.84 eV, while its HOMO can be finely tuned from −5.65 up to −5.10 eV by simply extending the oligothienyl π-bridge from 1T to 6T.[88] As the blended donor polymer was shifted from P3HT to the low bandgap PBDTTT-C-T, the photoactive layer may absorb more visible and even near infrared solar photons, leading to a dramatic increase of J_{sc}, and the lower lying LUMO of PBDTTT-C-T over P3HT contributes to a higher V_{oc}. As a result, both **PDI 6b**[41] and **6d**[89] gave a PCE of 4%. Using 2T-BDT-mediated diketopyrrolopyrrole (DPP) dimeric molecules as the donor materials, **PDI 6b** gave a PCE between 1.3 and 2.0%.[47,53] When the donor molecule was switched to high-efficiency *p*-DTS(FBTTh$_2$)$_2$, **PDI 6a** yielded a PCE of 3.7%.[90] Although the twisted dimeric conformation can improve the solution-processability and reduce the acceptor domain size close to the effective exciton diffusion length, the ordered packing of the dimeric molecules is compromised, and this leads to a lower electron mobility and increased recombination loss in the resulting solar cells. To improve the dimeric acceptor packing, Zhan, Yao and coworkers recently demonstrated that treatment of the photoactive layer with the vapour of the processing host solvent, *i.e.* 1,2-dicholobenzene (*o*-DCB), in a fully sealed Petri dish can significantly increase both the J_{sc} and FF values. This is because the slow evaporation of the host solvent is helpful for the acceptor molecules to self-organise and phase separate with the blend donor polymer, leading to the increase of electron mobility and reduction of recombination loss. Following such a solvent vapor annealing (SVA) process, the **PDI 6b**:PBDTTT-C-T system yielded an optimum PCE value of 6.1%.[91] Besides the film morphology in the photoactive layer, Zhan, Yao and coworkers developed a system based on a **PDI 6c**:PBDTTT-C-T combination and showed that the donor-to-acceptor compositions in the air and buried surfaces of the photoactive layer can be finely tuned with the amount of solvent additive, DIO, and it was found that the acceptor-to-donor abundance in the buried surface played a very important role in affecting the injection and extraction of the free electrons or holes, which then contributed to the cell's J_{sc} and FF.[92] By using indaceno[1,2-*b*:5,6-*b*′]dithiophene (IDT) as the aromatic π-bridge, Zhan and coworkers presented another solution-processable twisted PDI dimer (**PDI 9**), which showed a PCE of 3.1% when using a 2T-BDT-mediated DPP dimer as the donor material.[93] When the IDT was changed to the thienyl bridge, the resulting PDI dimer produced a PCE of 3.6% with PBDTTT-C-T as the donor polymer.[94] The different PCE values of 3.6% for this PDI dimer and the value of 6.1% achieved for **PDI 6b** with the same polymer as the donor and with an identical cell structure suggest that the additional oxygen atom from the 2-methoxylethoxyl group in **PDI 6b** could be important in realizing efficient NF-OSCs.

Pei, Zhao and coworkers reported a series of PDI dimers featuring arylene bay linkers, such as spirobifluorene-2,7′-diyl (**PDI 10**). This PDI dimer showed an absorption spectrum similar to that in solution, indicating minimal intermolecular aggregation in the thin film. The best inverted cell based on **PDI 10**:P3HT yielded a PCE of 2.35%.[43] As the blend donor material was changed into a high-efficiency polymer PffBT4T-2DT, Yan and coworkers reported that **PDI 10** achieved a PCE of 6.3%.[95] Wang and coworkers designed another series of bay-linked (singly, doubly and triply) PDI dimers featuring branched alkyl chains at the nitrogen positions. The bay-linked **PDI 11** enabled a PCE of 3.63%,[96] 4.39%,[97] 4.48%,[98] and 3.12%,[99] respectively utilizing PBDTTT-CT, PBDTBDD, PTB7-Th, and P(IID-DTC) as the blended polymer donor. A PCE of 5.90% was reported from blend of **PDI 11**:PTB7-Th using an inverted cell structure with a self-assembling monolayer of fullerene atop the ZnO interlayer.[100] During preparation of this review paper, Wang and coworkers reported another PDI dimer, **PDI 12**, with two S atoms fused on the bay region of the two PDI units. A PCE of 7.16% was achieved when blended with the polymer donor of PDBT-T1.[101] Nuckolls and coworkers designed a twisted PDI dimer formed by the fusion of two PDI units with a carbon–carbon double bond bridge (**PDI 13**), which achieved an efficiency of 6.05% when using PTB7-Th as the donor polymer and using 1% DIO plus 1% CN as the cosolvent additive.[102]

PDI trimer and tetramer. The spherical shape of the fullerene π-system is assumed to be capable of aligning with the donor π-plane in a three-dimensional (3-D) manner, which may decrease the Coulombic barrier for charge separation due to enhanced entropic effects and enables isotropic charge transport.[103] For this reason, PDI trimers and even tetramers with a 3-D structure were synthesized. Zhan, Yao and coworkers reported a star-shaped PDI trimer, **PDI 14**, in which three PDI units were covalently linked *via* a triphenylamine bridge (Fig. 11). This PDI trimer gave a PCE of 1.85% when blended with PBDTTT-C-T (Table 3).[104] Zhan and coworkers also presented a similar nonplanar, star-shaped PDI trimer, **PDI 15**, whose bay region was functionalized with butyloxyl side-chains. When using PBDTTT-C-T as the blended donor material, the device gave an optimum PCE of 3.22%.[105] Yan and coworkers reported a tetraphenylethylene (TPE) core-based PDI tetramer (**PDI 16**). Its four phenyl rings were highly twisted due to strong steric hindrance: they all tilted by about 50° relative to the plane of the central double bond and formed a "four-wing propeller-shape" molecular structure. Due to their highly twisted molecular structure, the TPE-based molecule exhibited weak intermolecular interactions and thus excellent solubility in organic solvents. In the blend with PTB7-Th, the best cell gave a PCE of 5.53%.[106] When the tetraphenylethylene core was changed into a tetraphenylmethane core, the resulting PDI tetramer (**17**) had a PCE of 4.3% using PffBT4T-2DT as the donor polymer.[107] This PCE value is lower than that from **PDI 10** also using PffBT4T-2DT as the donor. At the same time, Zhang and coworkers also designed another tetraphenylmethane-mediated PDI tetramer (**18**), which exhibited a PCE of 2.73% when using PBDTTT-C-T as the donor polymer.[108] From comparisons of the

 This journal is © The Royal Society of Chemistry 2015

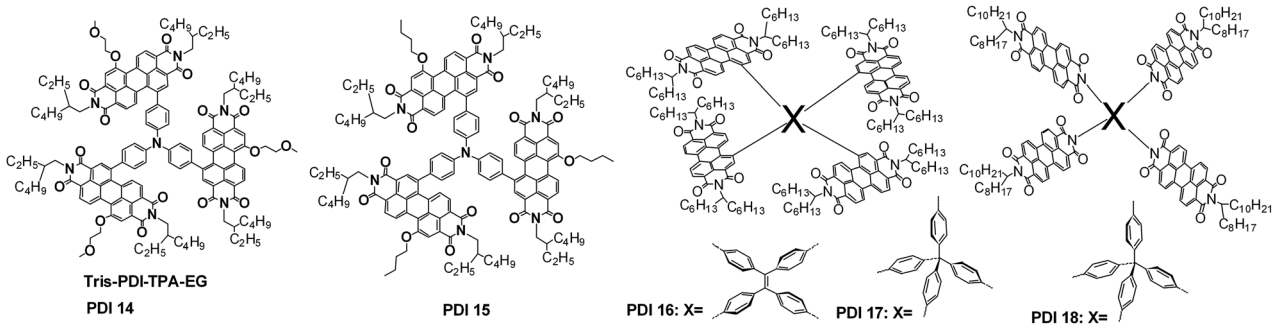

Fig. 11 Chemical structures of the PDI trimer and tetramer acceptors.

Table 3 Optoelectronic properties, electron–hole mobilities, and cell parameters from PDI 14–18

PDI	Donor	E_g^{opta} (eV)	LUMO/HOMO (eV)	μ_e/μ_h ($\times 10^{-3}$ cm^2 V^{-1} s^{-1})	J_{sc} (mA cm^{-2})	V_{oc} (V)	FF (%)	PCE^b (%)	Ref.
14	PBDTTT-C-T	1.71/1.58	−3.75/−5.60	—	5.89	0.91	34	1.85	104
15	PBDTTT-C-T	1.76/1.58	−3.70/−5.40	0.010/0.53	11.27	0.87	33	3.22	105
16	PTB7-Th	2.05/1.58	−3.72/−5.77	1/—	11.7	0.91	52	5.53	106
17	PffBT4T-2DT	2.25/1.55	−3.75/−6.00	0.28/—	9.2	0.96	49	4.3	107
18	PBDTTT-C-T	2.14/1.58	−3.82/−5.96	0.0018/0.056	7.83	0.77	45	2.73	108

[a] Optical bandgap obtained from the neat A and D film and presented in the manner of A/D. [b] Under illumination with AM 1.5G, 100 mW cm^{-2}.

Published on 08 2015. Downloaded on 06/08/2025 2:35:09 .

PCE values achieved from the trimer and tetramer of PDI and those from the PDI dimer, it seems that the PDI dimer can give a better cell performance when blended with the same donor molecule.

3.2. Non-PDI, large fused-ring π-system based small molecules

Pentacene is a typical p-type organic semiconductor, while octafluoropentacene derivatives such as **M1** with two silylethyne substituted groups, as shown in Fig. 12, have low-lying LUMO and HOMO levels, and can be used as non-fullerene acceptors, although they show an inferior performance when blended with a DPP-based small molecule donor (Table 4).[109] Wang and coworkers reported that quinacridone derivatives such as **M2**, which also contains five fused six-membered rings, gave a PCE value of 1.57% when it was blended with the commonly used donor polymer, P3HT.[110] Pei and coworkers reported a series of fluoranthene-fused imide derivatives, for example, **M3**. Their LUMO level could be tuned between −3.40 and −3.48 eV by changing the peripheral aryl substituted groups. Among them, that substituted with *o*-methylphenyl groups had a LUMO level of −3.43 eV and yielded a PCE value of 2.90% when using P3HT as the donor and following a solvent and subsequent thermal annealing process.[111,112] We noted that this PCE value of 2.90% was interesting because it was obtained by using a wide bandgap organic acceptor (2.83 eV) and the wide bandgap donor polymer P3HT.

Jenekhe and coworkers reported tetraazabenzodifluoranthene diimide (BFI) and bis(naphthalene imide)diphenylanthrazoline (BNIDPA) based organic acceptors. The conjugated benzodifluoranthene diimide can support efficient electron delocalization and polaron formation. The LUMO and HOMO energies of BNIDPA (**M5**) were both close to the values of the monomeric BFI (**M4**). However, the **M5**:PTB7-Th blend had a much higher electron mobility, and hence a much higher J_{sc} value than that of **M4**:PSEHTT (poly[(4,4′-bis(2-ethylhexyl)dithieno[3,2-*b*:2′,3′-*d*]silole)-2,6-diyl-*alt*-(2,5-bis(3-(2-ethylhexyl)-thiophen-2-yl)thiazolo[5,4-*d*]thiazole)]). **M5** gave a PCE value of 3%,[113] whereas **M4** only had a PCE of 1.5%.[114] When two BFI monomers were covalently linked together *via* a thienyl bridge, the resulting dimer, **M6a**, had a PCE of 5%, also due to the higher electron mobility and again the higher hole mobility.[114] The dihedral angle between the two BFI planes can be tuned up to 62° by using the 3,4-dimethylthienyl bridge. The resulting dimer can give an even higher J_{sc} value and a higher PCE of 6.2% was obtained.[115]

Indaceno[1,2-*b*:5,6-*b*0]dithiophene (IDT)[116] and indacenodithieno[3,2-*b*]thiophene (IDTT)[117] are two typical ladder-type electron-donating groups, in which the two thiophene/bithiophene subunits are covalently fastened to the central phenyl core *via* two sp^3 carbon atoms, forming coplanar large fused-ring π-systems. The four bulky *p*-(*n*-hexyl)aryl groups are introduced onto the sp^3 carbon atom as the peripheral substituents for tailoring the solution-processability. By covalently conjugating the electron-donating IDT or IDTT with the electron-accepting 2-(3-oxo-2,3-dihydroinden-1-ylidene) malononitrile, Zhan and coworkers reported two A–D–A based organic acceptors, **M7** and **M8**. When using PTB7-Th as the donor polymer and PDIN (a PDI monomer whose nitrogen positions were functionalized with 3-(*N*,*N*-dimethyl)propyl units)[118] as the cathode layer, **M7** and **M8** had a PCE of 6.31% and 6.80%, respectively.[119,120] Wudl and coworkers reported

Published on 08 2015. Downloaded on 06/08/2025 2:35:09 .

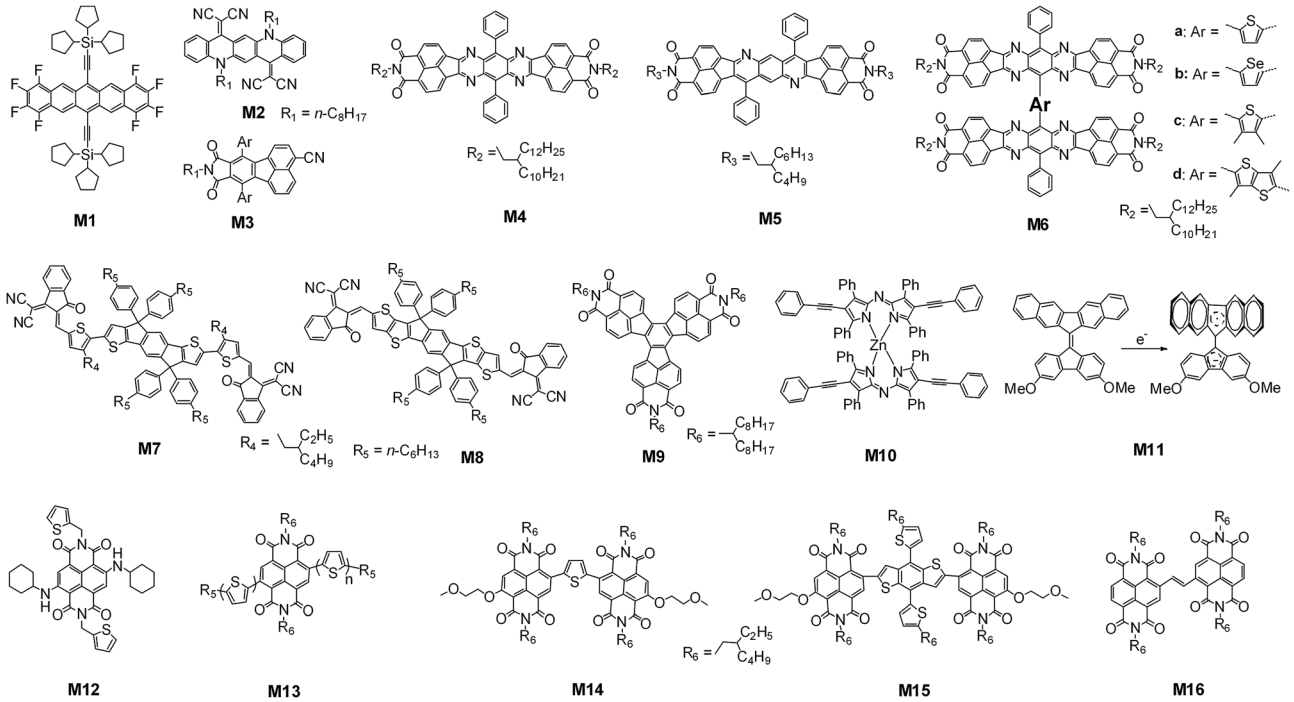

Fig. 12 Chemical structures of the typical reported non-PDI, large fused-ring π-system based small-molecule acceptors.

Table 4 Optoelectronic properties, electron–hole mobilities, and cell parameters for **M1–16**

Acceptor	Donor	E_g^{opta} (eV)	LUMO/HOMO (eV)	μ_e/μ_h ($\times 10^{-3}$ cm^2 V^{-1} s^{-1})	J_{sc} (mA cm^{-2})	V_{oc} (V)	FF (%)	PCE^b (%)	Ref.
M1	C6PT2C6	1.7^c/1.7^c	−3.71/−5.71	0.015/0.0015	0.66 ± 0.10	0.91 ± 0.13	45 ± 9	0.28 ± 0.10	109
M2	P3HT	1.8^c/2.0	−4.1/−5.9^d	0.11/—	5.72	0.48	57	1.57	110
M3	P3HT	2.83/2.0	−3.44/−6.27	0.009/0.15	6.35	0.95	48	2.90	112
M4	PSEHTT	2.2 ^{c}/1.65^c	−3.6/−5.8	0.00035/0.18	3.16	0.94	49	1.39 ± 0.05	114
M5	PTB7-Th	2.22/1.58	−3.6/−6.0	0.06/0.068	9.02	0.96	35	2.91 ± 0.08	113
M6a	PSEHTT	1.8^c/1.65^c	−3.8/−5.8	0.12/0.28	10.14	0.86	58	4.91 ± 0.13	114
M6c	PSEHTT	1.91/1.65^c	−3.70/−5.82	33.2/0.157	12.10 ± 0.36	0.91 ± 0.004	56 ± 1	6.18 ± 0.13	115
M7	PTB7-Th	1.57/1.58	−3.82/−5.42	0.10/0.45	13.05 ± 0.35	0.967 ± 0.002	47.3 ± 4	6.08 ± 0.20	119
M8	PTB7-Th	1.59/1.58	−3.83/−5.48	0.11/0.043	14.21	0.81	59	6.8	120
M9	P3HT	2.20/20	−3.61/−5.81	—	4.87	0.58	57	1.6	121
M10	P3HT	1.55/2.0	−3.85/−5.60	0.19/0.21	8.8 ± 0.5	0.76 ± 0.01	57 ± 3	3.90 ± 0.20	122
M11	P3HT	2.18/2.0	−3.24/−5.18	—	3.9	1.10	40	1.7	123
M12	P3HT	1.7^c/2.0	−3.71/−5.69	0.23/0.13	2.99 ± 0.09	0.70 ± 0.02	44 ± 1	0.94 ± 0.03	124
M13	P3HT	1.57/2.0	−4.05/−5.53	—	3.43	0.82	0.53	1.45	125
M14	PBDTTT-C-T	1.70/1.58	−3.80/−5.88	—	2.70	0.96	51	1.31	126
M15	PBDTTT-C-T	1.61/1.58	−3.78/−5.46	—	3.26	0.95	40	1.24	126
M16	PTB7	2.4^c/1.63	−4.35/−6.74	0.017/—	5.47	0.74	59.1	2.41	127

^{a} Optical bandgap obtained from the neat A and D film and presented in the manner of A/D. ^{b} Under illumination with AM 1.5G, 100 mW cm^{-2}. ^{c} Calculated from the absorption edge (λ_{edge}^{abs}) with the equation of $E_g^{opt} = 1240/\lambda_{edge}^{abs}$ (eV). The value of λ_{edge}^{abs} was obtained from the absorption spectrum presented in this reference. ^{d} Estimated using ultraviolet photoelectron spectroscopy (UPS) and optical bandgap data.

a coplanar, star-shaped decacyclene triimide based organic acceptor, **M9**, with three naphthaleneimide subunits fused with a central phenyl core. It had a PCE of 1.6% with P3HT as the blend polymer donor.[121]

Bis[2,6-diphenylethynyl-1,3,7,9-tetraphenylazadipyrromethene]zinc(II), **M10**, reported by Sauvé and coworkers, is an interesting non-fullerene acceptor in which the two azadipyrromethene planes are highly twisted with the conjugated arms pointing in four directions. Its low bandgap, intense absorption and low-lying LUMO and HOMO levels give it the potential to be applied as an electron accepting material. The best **M10**:P3HT blend based solar cell had a PCE of 4.10% and the control cell of the $PC_{61}BM$:P3HT blend had an optimum PCE of 3.7%.[122] Another interesting case is 9,9′-bifluorenylidene based derivatives, such as **M11**, reported by Wudl and coworkers. It was speculated that the addition of an electron across the 9,9′-double bond is highly favourable because of steric strain relief and a gain in aromaticity to form a 14-pi-

 This journal is © The Royal Society of Chemistry 2015

Published on 08 2015. Downloaded on 06/08/2025 2:35:09 .

electron system. Therefore, although **M11** had high-lying LUMO and HOMO energy levels (−3.24/−5.18 eV), it could act as an electron-accepting material and yielded a PCE of 1.7% when using P3HT as the donor.[123]

Naphthalene diimides (NDIs) are another kind of traditional n-type organic semiconductor. NDIs normally show an absorption band with an optical bandgap of 3 eV. One of the strategies to narrow the bandgap is to introduce electron-donating groups, favouring the intramolecular charge-transfer (ICT) transition from the peripheral unit to the NDI core. Recently, Sauvé and coworkers reported such an NDI derivative, **M12**, by introducing two *N*-cyclohexylamino groups onto the bay region of the NDI core. The resulting molecule had an optical bandgap down to 1.7 eV and its LUMO and HOMO energy levels were −3.71 and −5.69 eV, respectively. The ICT band is even stronger than the π–π* transition of the NDI core. Because the absorption of P3HT just follows between the ICT and the π–π* absorption of **M12**, the **M12**:P3HT blend thus had a wide solar spectrum coverage from 300 to 720 nm, and the solar cell based on this blend had an optimum PCE value of 1% after using 0.2% DIO as the additive and annealing below 100 °C for 1 h.[124] Jenekhe and coworkers reported another series of NDI monomer-based acceptors by covalently linking two oligothiophene units onto the 2 and 6-positions. The large oligothiophene size led to a red-shift of the onset of the resulting ICT absorption with the optical bandgap changing from 2.1 to 1.4 eV. Unfortunately, the ICT absorption was much weaker than the absorption of the NDI core. Of the molecules, **M13** had a PCE of 1.5% when using P3HT as the donor, TPBI as the cathode layer, 0.2% DIO as the additive and thermally annealing at 100 °C for 10 min.[125] Recently, Zhan and coworkers presented two NDI dimers, **M14** and **M15**, in which two NDI units were covalently linked with a bridge of thiophene or 2T-BDT. Compared to the thienyl bridged dimer, that mediated by 2T-BDT had a lower bandgap and its ICT absorption extended to 770 nm. However, the ICT absorption was still weak, which corresponded to a lower J_{sc}. When blended with PBDTTT-C-T, **M14** and **M15** yielded a V_{oc} of 0.95–0.96 V and PCE values of 1.31% and 1.24%, respectively.[126] Russell and coworkers synthesized another NDI dimer (**M16**) with a carbon–carbon double bond as the bridge. The **M16**:PTB7 blend based solar cell had an optimum PCE of 2.41% when using 0.5% DIO as the additive.[127]

3.3. Other conjugated π-system based small molecules

Compared to the PDI and non-PDI large fused-ring π-systems, there is another class of non-fullerene small-molecule acceptors which are normally constructed by covalently linking relatively small electron-donating and electron-accepting π-aromatics such as thiophene, benzene, vinazene, phthalimides, naphthalimides, thienoimide and indandione together. For these kinds of molecules, the formation of a coplanar backbone seems to be important for the achievement of high-efficiency charge transportation and electric performance.

Fréchet and coworkers reported that the 2-ethylhexyl dicyanoimidazol-2-yl (vinazene)-based molecule, **M17a** (Fig. 13), displayed an average PCE of 1.4% (Table 5) when it was blended with the polymer donor of poly[3-(4-*n*-octyl)phenylthiophene] (POPT).[128] When blended with a DPP based small molecular donor, which was terminated by benzofuran groups, **M17b** had a higher PCE of 1.10% than **M17a** (0.80%).[129] Sellinger and coworkers modified the molecular structure by replacing flanked vinazene with phthalimides or naphthalimides. The naphthalimide terminated molecule was typically amorphous in a solid film. However, the phthalimide terminated molecule (**M18**) showed significant crystallization in a spin-coated film and had a higher PCE value (2.54% *vs.* 0.12%) than the naphthalimide terminated molecule when mixed with P3HT. This was rationalised by **M18** possessing a more coplanar conjugated backbone, whereas the steric interactions between neighbouring hydrogen atoms in the naphthyl and vinyl moieties induced a 27.3° twist for the naphthalimide terminated backbone.[130] The PCE from the **M18**:P3HT based solar cell was further improved to 3.7% through optimization of the synthetic and purification procedures.[131] Fréchet and coworkers replaced the phthalimides with thienoimides and used a thienyl bridge instead of the CH=CH one, affording molecule **M19**. **M19** exhibited a broader absorption band and higher extinction coefficients than the phthalimide terminated control molecule, and had a higher PCE (2.4% *vs.* 0.85%) when blended with a DPP small molecule with perylene side-arms.[132]

Watkins and coworkers reported another different molecule, **M20**, in which a fluorene was end-capped with electron-accepting 2,3-dihydro-1*H*-indene-1,3-dione units *via* the thienyl bridge. The **M20**:P3HT based solar cell yielded a PCE of

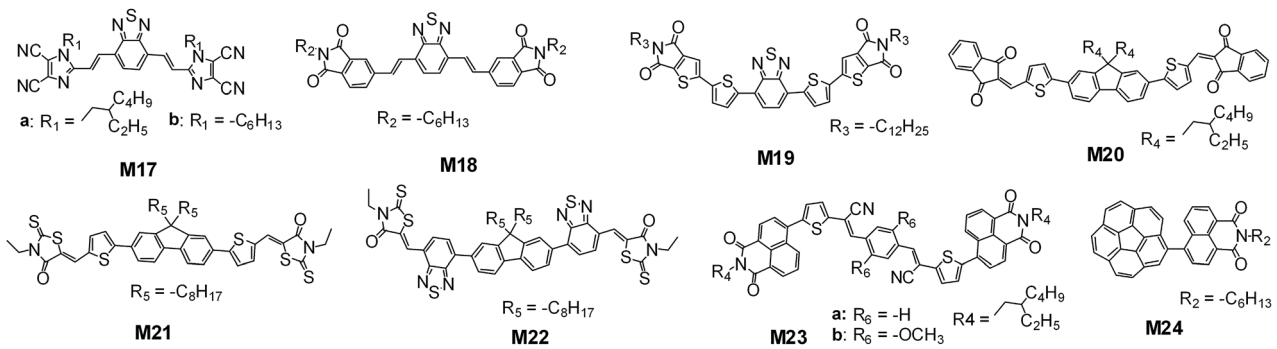

Fig. 13 Chemical structures of the reported typical small π-aromatic conjugation based small-molecule acceptors.

Table 5 Optoelectronic properties, electron–hole mobilities, and cell parameters from M17–24

Acceptor	Donor	$E_g^{opt a}$ (eV)	LUMO/HOMO (eV)	μ_e/μ_h ($\times 10^{-3}$ cm^2 V^{-1} s^{-1})	J_{sc} (mA cm^{-2})	V_{oc} (V)	FF (%)	PCE^b (%)	Ref.
M17a	POPT	2.43/1.8	−3.5/−6.0	—	5.50	0.62	40	1.41	128
M17b	DPP	2.43/1.75	−3.5/−6.0	0.063/—	2.76	1.08	37	1.10	129
M18	P3HT	2.34/2.0	−3.30/−5.77	—	4.7	0.96	56	2.54	130
M18	P3HT	2.34/2.0	−3.30/−5.77	—	6.5	0.94	61	3.7	131
M19	DPP-Py	1.89/1.72	−4.10/−5.99	—	3.72	1.05	60	2.33 ± 0.05	132
M20	P3HT	2.07^c/2.0	−3.95/−5.95		3.82	0.95	67	2.12 ± 0.18	133
M21	P3HT	1.55/2.0	−3.53/−5.58		5.7	1.03	52	3.08	134
M22	P3HT	2.14/2.0	−3.57/−5.70	0.026/—	7.95	0.82	63	4.11	135
M23a	P3HT	2.22/2.0	−3.42/−5.90	0.02/5.65 × 10^{-5}	8.04	0.73	46	2.51 ± 0.11	136
M23b	DTS(FBTTh$_2$)$_2$	2.22/1.55	−3.42/−5.90	0.175/0.0845	9.62 ± 0.269	0.85 ± 0.005	64 ± 1.4	5.30 ± 0.091	137
M24	P3HT	3.04/2.0	−3.24/—	0.132/—	2.75	0.82	46	1.03	138

^{a} Optical bandgap obtained from the neat A and D film and presented in the manner of A/D. ^{b} Under illumination with AM 1.5G, 100 mW cm^{-2}. ^{c} Calculated from the absorption edge (λ_{edge}^{abs}) with the equation of $E_g^{opt} = 1240/\lambda_{edge}^{abs}$ (eV). The value of λ_{edge}^{abs} was obtained from the absorption spectrum presented in this reference.

Published on 08 2015. Downloaded on 06/08/2025 2:35:09 .

2.4%.[133] Lim and coworkers replaced the indene-1,3-dione units with rhodanine, and synthesized a narrow bandgap molecule, **M21**, which had a PCE of 3.08%, also using P3HT as the donor.[134] Holliday and coworkers utilized the electron-accepting benzothiadiazole to replace the electron-donating thienyl bridge in **M21**. The resulting molecule **M22** had a PCE of 4.11%, again using P3HT as the donor.[135] Park and coworkers used two naphthalimide units to cap a dicyanodistyrylbenzene core with two thienyl bridges. The resulting molecules **M23a** and **M23b** had a PCE of 2.71% with P3HT as the donor[136] and a PCE of 5.44% with the low bandgap small molecule of *p*-DTS(FBTTh$_2$)$_2$ as the blended donor.[137] By covalently linking Corannulene with one naphthalimide unit, Cao and coworkers reported another molecule, **M24**, which had 1% efficiency using P3HT as the donor.[138]

3.4. Vacuum-deposited small molecules

Subphthalocyanines (SubPcs) are a class of phthalocyanine-related organic semiconductors (Fig. 14). A SubPc molecule consists of three instead of four diiminoisoindoline units, which are arranged around a boron atom.[139] In 2011, Torres, Heremans and coworkers reported a 2.5% efficiency vacuum deposited bilayered non-fullerene organic solar cell based on a fluorinated fused subphthalocyanine dimer and SubPc (**M26**). With the addition of a C_{60} layer atop the fluorinated fused dimer layer, an efficiency of 4% was obtained.[140] Bender and coworkers reported that the bilayer cell based on pentafluorophenoxy substituted boron subphthalocyanine (**M28**) (40 nm) and SubPc (10 nm) had an efficiency of 1% (Table 6).[141] The boron subnaphthalocyanine (**M27**) had a red-shifting absorption band and edge (730 nm), compared to **M26**. The absorption of the hexachloro-substituted SubPc **M29** was complementary to that of **M27**. Torres, Heremans and coworkers reported that a 6.4% efficiency was obtained from bilayered **M29**/**M27** using a blend of bathocuproine (BCP) and C_{60} as the cathode layer.[142] Recently, Heremans and coworkers achieved a PCE of 8.4% from a three-layered solar cell by exploiting the cascade energy transfer from a hexathiophene donor layer to the **M26** and **M27** layers.[143]

Sullivan and coworkers reported that a bilayered cell based on bis(diethyl-barbituric acid)-2,2′-bithiophene (**M30**) and **M26** had an efficiency of 1.3%.[144] Recently, Thompson and coworkers reported a zinc chlorodipyrrin based organic acceptor (**M31**). They demonstrated that the symmetry-broken zinc chlorodipyrrin was helpful to achieve a high V_{oc} value. The **M31**/tetraphenyldibenzoperyflanthrene cell had a V_{oc} of 1.33 V and the estimated CT state energy was 1.70 eV.[145] Nielsen and coworkers presented a star-shaped organic acceptor, **M32**. Compared to the mother unsubstituted truxenone core, the introduction of one, two and three ethyl cyanoacetate groups led to the truxenone core bending by 1.46°, 2.01°, and 2.68°, respectively. The best bilayered cell had a PCE of 1.30% with ZnPc as the donor layer.[146]

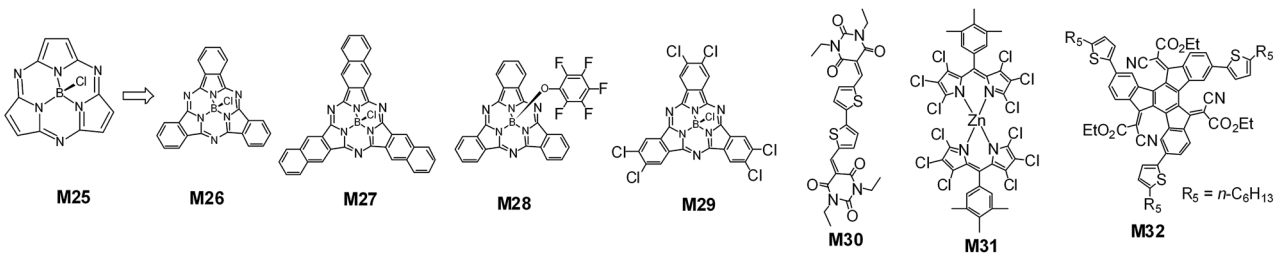

Fig. 14 Chemical structures of the reported vacuum-deposited small-molecule acceptors.

 This journal is © The Royal Society of Chemistry 2015

Table 6 Optoelectronic properties, electron–hole mobilities, and cell parameters from PDI 26–32

Acceptor	Donor	$E_g^{opt a}$ (eV)	LUMO/HOMO (eV)	J_{sc} (mA cm^{-2})	V_{oc} (V)	FF (%)	PCE^b (%)	Ref.
M28	**M26**	—/1.9	−3.6/−5.7	2.06 ± 0.71	1.06 ± 0.03	43.2 ± 0.9	0.94 ± 0.33	141
M29	**M27**	—/1.7	—	9.0	1.03	71	6.4	142
M26/**M27**	α-6T	1.9^c/1.7/2.17^c	—	14.55	0.96	61.0	8.40	143
M30	**M26**	2^c/1.9	−4.23/−6.28	2.34	1.38	40	1.28	144
M31	ZnPc	2.10/—	−3.88/−6.0	3.45	0.59	63	1.30	145
M32	DBP	2.07^c/1.9	−4.10/−6.4^d	6.2	0.88	68	3.6	146

^{a} Optical bandgap obtained from the neat A and D film and presented in the manner of A/D. ^{b} Under illumination with AM 1.5G, 100 mW cm^{-2}. ^{c} Calculated from the absorption edge (λ_{edge}^{abs}) with the equation of $E_g^{opt} = 1240/\lambda_{edge}^{abs}$ (eV). The value of λ_{edge}^{abs} was obtained from the absorption spectrum presented in the reference. ^{d} Estimated using ultraviolet photoelectron spectroscopy (UPS) and optical bandgap data.

Published on 08 2015. Downloaded on 06/08/2025 2:35:09 .

4. Polymer non-fullerene acceptors

D–A conjugation is a general strategy to polymer acceptors. Similarly to the small molecules, the rylene diimide based systems are widely investigated polymer acceptors. Bao, Zhao and coworkers reported 4.21% efficiency from a PDI-thiophene based polymer acceptor, **P1** (Fig. 15), with an isoindigo-bithiophene based polymer (PiI-2T-PS5) as the blended donor material (Table 7).[147] When using P3HT as the donor, the PDI-bithiophene based polymer (**P2**) had a PCE of 2.17%.[148] Zhan and coworkers reported the PDI-dithienothiophene based polymer (**P3**) in 1997, which had a PCE of 1% using bi(thienylenevinylene)-substituted polythiophene as the donor.[52] The same polymer acceptor had a PCE of 3.45% when using PBDTTT-C-T as the donor and a PDI derivative as the additive.[149] Yu and coworkers used an electron-accepting moiety, 4,10-bis(2-butyloctyl)thieno[2′,3′:5,6]pyrido[3,4-*g*]thieno-[3,2-*c*]isoquinoline-5,11-dione (TPTI),[150] instead of an electron-donating unit to conjugate the PDI chromophore. The resulting polymer acceptor had a PCE of 1% when PTB7 was used as the donor material.[151] When TPTI was replaced with its isomer, 5,11-bis(2-butyloctyl)dihydrothieno[2′,3′:4,5]pyrido[2,3-*g*]thieno [3,2-*c*]quinoline-4,10-dione (TPTQ), the resulting polymer acceptor, **P4**, had a PCE of 3.22% when blended with PTB7-Th.[152] The LUMO energy level of PDI based polymers was normally in the region of −3.8 to −4.0 eV. When two thienyl units were fused with the 1,12- and 6,7-positions of the PDI core,[153] or the diimide functionalities were converted into tetracarboxylic tetraester groups,[154] the LUMO energy of the resulting PDI polymer could be up to about −3.5 eV.

NDI based polymers are another interesting class of polymer acceptors. Recently, Kim and coworkers used thiophene as the conjugated electron-donating moiety and reported a NDI-thiophene based polymer, **P5**, which had a PCE of 6% when blended with PTB7-Th.[155] Based on **P5**, Kim, Yoo and coworkers demonstrated that the polymer donor weight of PPDT2FBT had a significant effect on the polymer aggregation and phase segregation, and, hence the electric performance of the all-polymer organic solar cell. From this D–A system, they found that a high molecular weight can afford the most efficient cell device.[156] Jenekhe and coworkers reported a NDI-selenophene based polymer, **P6**, which had a PCE value of 3.3% [157] and 7.7% [46] when using PSEHTT and PTB7-Th as the polymer donor, respectively. The NDI-bithiophene based polymer, **P7**, is commercially available. A PCE value of 6.4% was published by Polyera for this polymer acceptor in 2013.[12] The non-fullerene small molecular organic solar cells (NF-SMSCs) based on the blends of **P7** (polymer acceptor) and small molecule donors such as *p*-DTS(FBTTh$_2$)$_2$[158,159] or electron-donating moiety-mediated DPP dimers[160,161] showed a PCE value of 2–5%. The all-polymer organic solar cells (all PSCs) with **P7** as the polymer acceptor exhibited a PCE of 2–5.5%, with polymers such as PTB7,[162] PTQ1 (poly[2,3-bis(3-octyloxyphenyl)quinoxaline-5,8-diyl-*alt*-thiophene-2,5-diyl]),[163] BFS4 (a dithienyl-benzo[1,2-*b*:4,5-*b*]dithiophene/5-fluoro-2,1,3-benzothiadiazole co-polymer),[164] NT (a naphthobisthiadiazole-benzodithiophene co-polymer),[165] and PTB7-Th[166] used as the donor material,

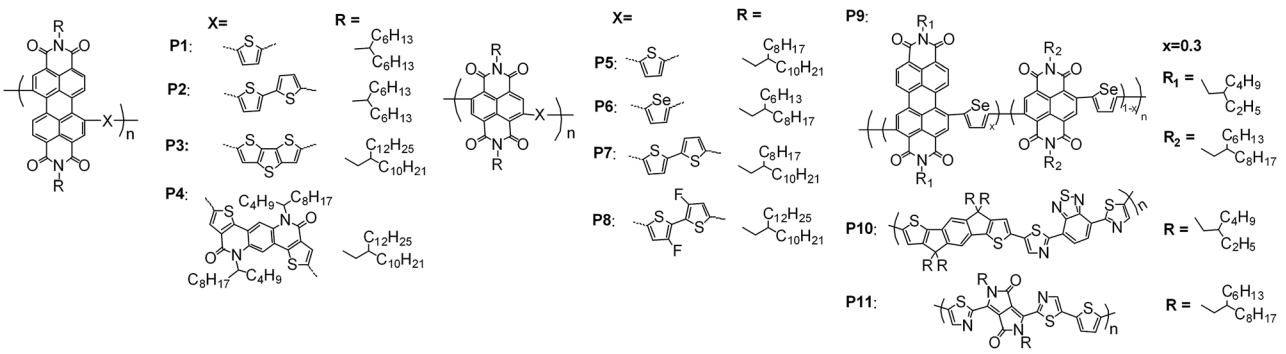

Fig. 15 Chemical structures of the typical reported PDI, NDI and other electron-accepting unit based polymer acceptors.

Table 7 Optoelectronic properties, electron–hole mobilities, and cell parameters for polymer acceptors P1–P11

A	D	Mn[a] (kDa)	PDI[b]	E_g^{optc} A/D (eV)	LUMO/HOMO (eV)	μ_e/μ_h ($\times 10^{-3}$ cm^2 V^{-1} s^{-1})	J_{sc} (mA cm^{-2})	V_{oc} (V)	FF (%)	PCE[d] (%)	Ref.
P1	PiI-2T-PS5	20.5	2.1	1.8/1.6	−3.80[f]/−5.72[g]	0.02/0.2	8.77 ± 0.29	1.04 ± 0.01	46 ± 1	4.21 ± 0.10	147
P2	P3HT	15.1	1.81	1.7[e]/2.0	−3.8/−5.5	0.5/—	7.65	0.52	55	2.17	148
P3	PBDTTT-C-T	—	—	—/1.58	−3.9/−5.9	0.0135/—	8.55	0.752	51.5	3.45	149
P4	PTB7-Th	21.6	2.83	1.74/1.58	−3.97/−5.97	0.11/0.84	7.72 ± 0.12	0.70 ± 0.01	57 ± 0.8	3.08 ± 0.14	152
P5	PTB7-Th	48.2	2.1	1.85/1.58	3.79/−5.64	0.084/0.28	13.46	0.79	56	5.96	155
P6	PTB7-Th	28.4	1.5	1.76/1.59	−3.84/−6.0	7.25/0.274	18.61 ± 0.21	0.80 ± 0.00	48 ± 1	7.21 ± 0.24	46
P7	DTP-DPP	—	—	1.45/1.52	−4.1/−5.7	—/—	10.14	0.82	58	4.82	161
P7	PTB7-Th	—	—	1.38[e]/1.58	−4.3/−5.9	4.1/0.96	13.0 ± 0.22	0.795 ± 0.00	53.4 ± 0.1	5.50 ± 0.08	166
P8	PTB7-Th	41.4	1.6	1.55[e]/1.58	−3.9/−5.8	0.49/0.55	13.53	0.81	62	6.71	167
P9	PBDTTT-C-T	37.5	1.4	1.77/1.58	−3.9/−5.95	1.0/2.6	18.22 ± 0.28	0.78 ± 0.002	43 ± 1	6.17 ± 0.10	172
P10	P3HT	14.3	1.82	1.98/2.0	−3.45/−5.43	—/—	2.6	1	0.45	1.18	174
P11	PDDP5T	93.3	3.05	1.44/1.30	−4.00/−5.63	—/—	6.9	0.81	0.51	2.9	175

[a] Number-average molecular weight of the polymer acceptor. [b] Polydispersity index of the polymer acceptor. [c] Optical bandgap obtained from the neat D and A film and presented in the manner of A/D. [d] Under illumination wit AM 1.5G, 100 mW cm^{-2}. [e] Calculated from the absorption edge (λ_{edge}^{abs}) with the equation of $E_g^{opt} = 1240/\lambda_{edge}^{abs}$ (eV). The value of λ_{edge}^{abs} was obtained from the absorption spectrum presented in this reference. [f] By inverse photoemission spectroscopy (IPES). [g] By UPS.

Published on 08 2015. Downloaded on 06/08/2025 2:35:09 .

respectively. By fluorinating the bithiophene unit in **P7** and further converting the side-chains on the NDI units into 2-decyltetradecyl, Jen and coworkers reported a new NDI-bithiophene based copolymer, **P8**, from which a PCE of 6.7% was obtained with PTB7-Th as the polymer donor.[167] Other NDI based polymer acceptors, with thienylene–vinylene–thienylene[168] and *N*-(1-octylnonyl)carbazole,[169] for example, as the conjugated electron-donating unit were reported to have a PCE of 4.3% and 3.7%, respectively, with PTB7-Th and another low-bandgap co-polymer of VVT7 as the donor material. Besides this, naphthobisthiazole diimide based copolymers were synthesized and investigated as polymer acceptors with PSEHTT as the donor, giving an optimum PCE of 1.4%.[170] With respect to the NDI-selenophene/NDI-selenophene random copolymer (with 2-butyloctyl and 2-decyltetradecyl on the NDI nitrogen positions, respectively),[171] the PDI-selenophene/NDI-selenophene random copolymer (**P9**) had a higher electron and hole mobility when blended with PBDTTT-C-T, and a PCE of 6.3% was obtained.[172] When carbazole was selected as the electron-donating unit, the resulting PDI–NDI random copolymer had a very inferior electric performance with a PCE of <0.5%.[173]

Otherwise, there have been reported several non-PDI or non-NDI based copolymer acceptors such as the dithiazolyl-benzothiadiazole based **P10** and the DPP-thiazole based **P11**, which had a PCE of 1.2% [174] and 2.9%,[175] respectively, with P3HT and the DPP-terthiophene copolymer as the donor material.

5. Challenges in NF-OSCs

Nowadays, among the four parameters from solution-processed NF-OSCs, the V_{oc} value can be up to 0.8–1.1 V, comparable to those of perovskite solar cells, which are typically about 1 V, but much higher than that of the corresponding fullerene solar cells. The J_{sc} value can be up to 13 mA cm^{-2}, and even up to 18–19 mA cm^{-2}.[46,172] The high J_{sc} values of 18–19 mA cm^{-2} have become comparable to those of high-efficiency fullerene organic solar cells, typically 18–20 mA cm^{-2}.[5,6,24–37] While the FF value is normally smaller than 60%, some of cells can have a higher FF value, approaching about 65%. It can be seen that the FF value from NF-OSCs is much smaller than the value of the high-efficiency fullerene organic solar cells, typically up to 70–80%. Therefore, improving the FF value is a key issue in designing high-efficiency NF-OSCs that can compete with their fullerene counterparts.

The FF value is relative to the recombination losses, carrier mobility and lifetime, *etc.* Meanwhile, the J_{sc} is scaled by the recombination losses and carrier mobility and lifetime, and it is also related to the light absorption ability of the donor–acceptor materials. As we can see from the above parts, the donor-to-acceptor combination and film morphology optimization are both important for high J_{sc}, FF and even V_{oc} values. From Tables 1–5 and 7, we can see that the electron mobility from most reported donor-to-acceptor systems is normally smaller than the corresponding hole mobility measured from the same blend film. In this context, designing acceptor materials with an improved electron mobility is required. However, the current design concept, for example, for the most efficient PDI and non-PDI large fused ring π-system based small molecule acceptors, is to compromise the crystallinity and the solution-processability, for example, to achieve nanoscale phase domains. The electron-mobility is therefore traded off. Designing new acceptor molecules with an ideal electron mobility is a big challenge to date.

Non-geminate loss of the CT state should be another focus. The donor-to-acceptor arrangement at the interface is an important factor in influencing charge separation. Cvetko, Morgante and coworkers indicated that a donor molecule with shape-complementarity to the spherical PCBM may have an extended interface between the donor and acceptor molecules, leading to faster electron transfer from the donor to the PCBM.[65] McGehee, Beaujuge, and coworkers reported that the intermolecular arrangement of the donor and PCBM can be

 This journal is © The Royal Society of Chemistry 2015

Published on 08 2015. Downloaded on 06/08/2025 2:35:09 .

adjusted by the positions of the branched and linear alkyl side chains either on the D or A moiety of the conjugated backbone of the polymer donor: the steric effects from the 2-ethylhexyl side chain on the D unit (with the linear one on the A moiety) hinder interactions of the D unit with the fullerene while the fullerene docks with the A moiety, presenting a higher cell performance.[66] Fréchet, Brédas and coworkers showed that introducing the twisted octylphenyl side group instead of a linear alkyl one on the polythiophene backbone decreases the barrier to the charge separation (for example, with the enlargement of the donor–acceptor distance), leading to a higher efficiency.[67] Zhan and coworkers demonstrated that the capped diphenylamine can improve the donor-to-acceptor compatibility through the π–π interactions between the diphenylamine group and $PC_{71}BM$, with respect to the butyl capped alkyl chain, and thus, enhance the charge separation and G_{max}^{e-h} value.[68] However, effects of the donor-to-acceptor interfacial structures on the charge separation is less known to date. Deeper understanding of these effects is urgently needed and is another big challenge in the development of high-efficiency non-fullerene organic solar cells or even fullerene organic solar cells, in particular, on the basis of ultrafast-absorption-spectrum-data.

6. Conclusions

Since 2013, fast advances have been achieved in NF-OSCs, a subbranch of organic solar cells. These advances include the judicious design and synthesis of new acceptor molecules, realization of new efficient donor–acceptor combinations, studying the role of the acceptor domain morphology and structural order in the cell performance. Along with such great efforts, the efficiency of NF-OSCs has been raised from 4% up to 8% in a short 3 year period of time. Among these advances, several kinds of small molecule and polymer acceptors have been investigated. The reported small-molecules include those based on perylene diimide, non-perylene diimide large π-fused rings and other conjugated systems from relatively small electron donating and accepting π-aromatics. Of the polymer acceptors, current interest is focused on the perylene diimide based polymer, while other polymers utilizing DPP or benzothiadiazole as the electron-accepting units have also been studied.

Although fast advances have been achieved, the reported efficiency of NF-OSCs as yet lags behinds their fullerene counterparts. One of the major obstacles is the relatively low electron mobility and strong recombination losses. Finding ways towards improving the electron mobility and suppressing recombination losses through the acceptor molecule design, film morphology optimization, and organic–electrode interface engineering, for example, are necessary to realize efficient NF-OSCs. Both low electron mobility and strong recombination loss significantly limit the cell's FF value. Recently, Neher, Koster and coworkers introduced a dimensionless parameter to quantify the ratio of recombination and extraction rates, showing improvements of charge transportation, while reduction of the charge recombination loss is needed to achieve a high FF value.[176]

Organic acceptors are much richer in source than fullerene ones. Chemical modifications on organic molecules are more accessible, and hence, the tuning of the absorption, either blue or red shifting, and energy levels, either going to high- or low-lying levels, are more available on organic π-systems than on fullerene systems. This accompanies the achievements in the synthesis of high-efficiency donor molecules. Even high efficiency NF-OSCs can be expected in the near future and NF-OSCs will become competitive with their fullerene counterparts.

Acknowledgements

This work was financially supported by NSFC (No. 21327805, 91227112, 91433202 and 21221002), and Chinese Academy of Sciences (XDB12010200).

Notes and references

1 *2013 Renewable Energy Data Book*, http://www.nrel.gov/.
2 M. A. Green, K. Emery, Y. Hishikawa, W. Warta and E. D. Dunlop, Solar cell efficiency tables (Version 45), *Prog. Photovoltaics*, 2015, **23**, 1–9.
3 G. Yu, J. Gao, J. C. Hummelen, F. Wudl and A. J. Heeger, Polymer photovoltaic cells: Enhanced efficiencies via a network of internal donor–acceptor heterojunctions, *Science*, 1995, **270**, 1789–1791.
4 C. W. Tang, Two-layer organic photovoltaic cell, *Appl. Phys. Lett.*, 1986, **48**, 183–185.
5 Y. Liu, J. Zhao, Z. Li, C. Mu, W. Ma, H. Hu, K. Jiang, H. Lin, H. Ade and H. Yan, Aggregation and morphology control enables multiple cases of high-efficiency polymer solar cells, *Nat. Commun.*, 2014, **5**, 5293.
6 A. R. B. M. Yusoff, D. Kim, H. P. Kim, F. K. Shneider, W. J. da Silva and J. Jang, High efficiency solution processed polymer inverted triple-junction solar cell exhibiting conversion efficiency of 11.83%, *Energy Environ. Sci.*, 2015, **8**, 303–316.
7 J. E. Anthony, Small-Molecule, Nonfullerene Acceptors for Polymer Bulk Heterojunction Organic Photovoltaics, *Chem. Mater.*, 2011, **23**, 583–590.
8 Y. Shu, Y.-F. Lim, Z. Li, B. Purushothaman, R. Hallani, J. E. Kim, S. R. Parkin, G. G. Malliaras and J. E. Anthony, A survey of electron-deficient pentacenes as acceptors in polymer bulk heterojunction solar cells, *Chem. Sci.*, 2011, **2**, 363–368.
9 P. Sonar, J. P. F. Lim and K. L. Chan, Organic non-fullerene acceptors for organic photovoltaics, *Energy Environ. Sci.*, 2011, **4**, 1558–1574.
10 E. Kozma and M. Catellani, Perylene diimides based materials for organic solar cells, *Dyes Pigm.*, 2013, **98**, 160–179.
11 C. L. Chochos, N. Tagmatarchisc and V. S. G. Gregoriou, Rational design on n-type organic materials for high performance organic photovoltaics, *RSC Adv.*, 2013, **3**, 7160–7181.
12 A. Facchetti, Polymer donor–polymer acceptor (all-polymer) solar cells, *Mater. Today*, 2013, **16**, 123–132.

Published on 08 2015. Downloaded on 06/08/2025 2:35:09 .

13 P. Hudhomme, An overview of molecular acceptors for organic solar cells, *EPJ Photovoltaics*, 2013, **4**, 40401.
14 A. F. Eftaiha, J.-P. Sun, I. G. Hill and G. C. Welch, Recent advances of non-fullerene, small molecular acceptors for solution processed bulk heterojunction solar cells, *J. Mater. Chem. A*, 2014, **2**, 1201–1213.
15 Y. Kim and E. Lim, Development of Polymer Acceptors for Organic Photovoltaic Cells, *Polymers*, 2014, **6**, 382–407.
16 Y. Lin and X. Zhan, Non-fullerene acceptors for organic photovoltaics: an emerging horizon, *Mater. Horiz.*, 2014, **1**, 470–488.
17 C. Li and H. Wonneberger, Perylene Imides for Organic Photovoltaics: Yesterday, Today, and Tomorrow, *Adv. Mater.*, 2012, **24**, 613–636.
18 M.-E. Ragoussia and T. Torres, New generation solar cells: concepts, trends and perspectives, *Chem. Commun.*, 2015, **51**, 3957–3972.
19 C. L. Zhan and A. D. Q. Li, Perylene Diimide: Versatile Building Blocks for Molecular Self-Assemblies, Folding Motifs, and Reaction-Directing Codes, *Curr. Org. Chem.*, 2011, **15**, 1314–1339.
20 F. Wang, Z. Tan and Y. Li, Solution-processable metal oxides/chelates as electrode buffer layers for efficient and stable polymer solar cells, *Energy Environ. Sci.*, 2015, **8**, 1059–1091.
21 S. Braun, W. R. Salaneck and M. Fahlman, Energy-Level Alignment at Organic/Metal and Organic/Organic Interfaces, *Adv. Mater.*, 2009, **21**, 1450–1472.
22 L. Lu and L. Yu, Understanding Low Bandgap Polymer PTB7 and Optimizing Polymer Solar Cells Based on It, *Adv. Mater.*, 2014, **26**, 4413–4430.
23 S.-H. Liao, H.-J. Jhuo, Y.-S. Cheng and S.-A. Chen, Fullerene Derivative-Doped Zinc Oxide Nanofilm as the Cathode of Inverted Polymer Solar Cells with Low-Bandgap Polymer (PTB7-Th) for High Performance, *Adv. Mater.*, 2013, **25**, 4766–4771.
24 V. Gupta, A. K. K. Kyaw, D. H. Wang, S. Chand, G. C. Bazan and A. J. Heeger, Barium: An Efficient Cathode Layer for Bulk-heterojunction Solar Cells, *Sci. Rep.*, 2013, **3**, 1965.
25 B. Kan, M. Li, Q. Zhang, F. Liu, X. Wan, Y. Wang, W. Ni, G. Long, X. Yang, H. Feng, Y. Zuo, M. Zhang, F. Huang, Y. Cao, T. P. Russell and Y. Chen, A Series of Simple Oligomer-like Small Molecules Based on Oligothiophenes for Solution-Processed Solar Cells with High Efficiency, *J. Am. Chem. Soc.*, 2015, **137**, 3886–3893.
26 S. Zhang, L. Ye, W. Zhan, B. Yang, Q. Wang and J. Hou, Realizing Over 10% Efficiency in Polymer Solar Cell by Device Optimization, *Sci. China: Chem.*, 2015, **58**, 248–256.
27 J.-D. Chen, C. Cui, Y.-Q. Li, L. Zhou, Q.-D. Ou, C. Li, Y. Li and J.-X. Tang, Single-Junction Polymer Solar Cells Exceeding 10% Power Conversion Efficiency, *Adv. Mater.*, 2015, **27**, 1035–1041.
28 Z. He, B. Xiao, F. Liu, H. Wu, Y. Yang, S. Xiao, C. Wang, T. P. Russell and Y. Cao, Single-junction polymer solar cells with high efficiency and photovoltage, *Nat. Photonics*, 2015, **9**, 174–179.
29 J. Zhang, Y. Zhang, J. Fang, K. Lu, Z. Wang, W. Ma and Z. Wei, Conjugated polymer-small molecule alloy leads to high efficient ternary organic solar cells, *J. Am. Chem. Soc.*, 2015, **137**, 8176–8183.
30 W. Yu, L. Huang, D. Yang, P. Fu, L. Zhou, J. Zhang and C. Li, Efficiency exceeding 10% for inverted polymer solar cells with ZnO/ionic liquid combined cathode interfacial layer, *J. Mater. Chem. A*, 2015, **2015**(3), 10660–10665.
31 S. Liu, P. You, J. Li, J. Li, C.-S. Lee, B. S. Ong, C. Surya and F. Yan, Enhanced efficiency of polymer solar cells by adding a high-mobility conjugated polymer, *Energy Environ. Sci.*, 2015, **8**, 1463–1470.
32 J. Huang, C.-Z. Li, C.-C. Chueh, S.-Q. Liu, J.-S. Yu and A. K.-Y. Jen, 10.4% Power Conversion Efficiency of ITO-Free Organic Photovoltaics Through Enhanced Light Trapping Configuration, *Adv. Energy Mater.*, 2015, 1500406.
33 L. K. Jagadamma, M. Al-Senani, A. El-Labban, I. Gereige, G. O. N. Ndjawa, J. C. D. Faria, T. Kim, K. Zhao, F. Cruciani, D. H. Anjum, M. A. McLachlan, P. M. Beaujuge and A. Amassian, Polymer Solar Cells with Efficiency >10% Enabled *via* a Facile Solution-Processed Al-Doped ZnO Electron Transporting Layer, *Adv. Energy Mater.*, 2015, 1500204.
34 V. Vohra, K. Kawashima, T. Kakara, T. Koganezawa, I. Osaka, K. Takimiya and H. Murata, Efficient inverted polymer solar cells employing favourable molecular orientation, *Nat. Photonics*, 2015, **9**, 403–408.
35 X. Ouyang, R. Peng, L. Ai, X. Zhang and Z. Ge, Efficient polymer solar cells employing a non-conjugated small-molecule electrolyte, *Nat. Photonics*, 2015, **9**, 520–524.
36 L. Zuo, C.-Y. Chang, C.-C. Chueh, S. Zhang, H. Li, A. K.-Y. Jen and H. Chen, Design of a versatile interconnecting layer for highly efficient series-connected polymer tandem solar cells, *Energy Environ. Sci.*, 2015, **8**, 1712–1718.
37 H. Zhou, Y. Zhang, C.-K. Mai, S. D. Collins, G. C. Bazan, T.-Q. Nguyen and A. J. Heeger, Polymer Homo-Tandem Solar Cells with Best Efficiency of 11.3%, *Adv. Mater.*, 2015, **27**, 1767–1773.
38 Y. Li, Molecular Design of Photovoltaic Materials for Polymer Solar Cells: Toward Suitable Electronic Energy Levels and Broad Absorption, *Acc. Chem. Res.*, 2012, **45**, 723–733.
39 E. Zhou, J. Cong, Q. Wei, K. Tajima, C. Yang and K. Hashimoto, All-Polymer Solar Cells from Perylene Diimide Based Copolymers: Material Design and Phase Separation Control, *Angew. Chem., Int. Ed.*, 2011, **50**, 2799–2803.
40 J. T. Bloking, X. Han, A. T. Higgs, J. P. Kastrop, L. Pandey, J. E. Norton, C. Risko, C. E. Chen, J.-L. Brédas, M. D. McGehee and A. Sellinger, Solution-Processed Organic Solar Cells with Power Conversion Efficiencies of 2.5% using Benzothiadiazole/Imide-Based Acceptors, *Chem. Mater.*, 2011, **23**, 5484–5490.
41 X. Zhang, Z. H. Lu, L. Ye, C. L. Zhan, J. Hou, S. Zhang, B. Jiang, Y. Zhao, J. H. Huang, S. L. Zhang, Y. Liu, Q. Shi, Y. Liu and J. N. Yao, A Potential Perylene Diimide Dimer-

 This journal is © The Royal Society of Chemistry 2015

Published on 08 2015. Downloaded on 06/08/2025 2:35:09 .

Based Acceptor Material for Highly Efficient Solution-Processed Non-Fullerene Organic Solar Cells with 4.03% Efficiency, *Adv. Mater.*, 2013, **25**, 5791–5797.

42 R. Shivanna, S. Shoaee, S. Dimitrov, S. K. Kandappa, S. Rajaram, J. R. Durrant and K. S. Narayan, Charge Generation and Transport in Efficient Organic Bulk Heterojunction Solar Cells with a Perylene Acceptor, *Energy Environ. Sci.*, 2014, **7**, 435–441.

43 Q. F. Yan, Y. Zhou, Y. Q. Zheng, J. Pei and D. H. Zhao, Towards Rational Design of Organic Electron Acceptors for Photovoltaics: a Study Based on Perylenediimide Derivatives, *Chem. Sci.*, 2013, **4**, 4389–4394.

44 B. Jiang, X. Zhang, C. L. Zhan, Z. H. Lu, J. H. Huang, X. L. Ding, S. G. He and J. N. Yao, Benzodithiophene Bridged Dimeric Perylene Diimide Amphiphile as Efficient Solution-Processed Non-Fullerene Small Molecule, *Polym. Chem.*, 2013, **4**, 4631–4638.

45 Z. H. Lu, X. Zhang, C. L. Zhan, B. Jiang, X. L. Zhang, L. L. Chen and J. N. Yao, Impact of Molecular Solvophobicity *vs.* Solvophilicity on Device Performances of Dimeric Perylene Diimide Based Solution-Processed Non-Fullerene Organic Solar Cells, *Phys. Chem. Chem. Phys.*, 2013, **15**, 11375–11385.

46 Y.-J. Hwang, B. A. E. Courtright, A. S. Ferreira, S. H. Tolbert and S. A. Jenekhe, 7.7% Efficient All-Polymer Solar Cells, *Adv. Mater.*, 2015, **27**, 4578–4584.

47 J. H. Huang, X. Wang, X. Zhang, Z. X. Niu, Z. H. Lu, B. Jiang, Y. X. Sun, C. L. Zhan and J. N. Yao, Additive-Assisted Control over Phase-Separated Nanostructures by Manipulating Alkylthienyl Position at Donor Backbone for Solution-Processed Non-Fullerene All-Small-Molecule Solar Cells, *ACS Appl. Mater. Interfaces*, 2014, **6**, 3853–3862.

48 Y. He, H. Chen, J. Hou and Y. Li, Indene–C_{60} Bisadduct: A New Acceptor for High-Performance Polymer Solar Cells, *J. Am. Chem. Soc.*, 2010, **132**, 1377–1382.

49 A. Anctil, C. W. Babbitt, R. P. Raffaelle and B. J. Landi, Material and Energy Intensity of Fullerene Production, *Environ. Sci. Technol.*, 2011, **45**, 2353–2359.

50 X. Zhang, C. L. Zhan and J. N. Yao, Non-Fullerene Organic Solar Cells with 6.1% Efficiency through Fine-Tuning Parameters of Film-Forming Process, *Chem. Mater.*, 2015, **27**(1), 166–173.

51 H. K. H. Lee, Z. Li, I. Constantinou, F. So, S. W. Tsang and S. K. So, Batch-to-Batch Variation of Polymeric Photovoltaic Materials: its Origin and Impacts on Charge Carrier Transport and Device Performances, *Adv. Energy Mater.*, 2014, 1400768.

52 X. Zhan, Z. Tan, B. Domercq, Z. An, X. Zhang, S. Barlow, Y. Li, D. Zhu, B. Kippelen and S. R. Marder, A High-Mobility Electron-Transport Polymer with Broad Absorption and Its Use in Field-Effect Transistors and All-Polymer Solar Cells, *J. Am. Chem. Soc.*, 2007, **129**, 7246–7247.

53 Y. X. Chen, A. L. Tang, X. Zhang, Z. L. Lu, J. H. Huang, C. L. Zhan and J. N. Yao, A New Solution-Processed Diketopyrrolopyrrole Donor for Non-Fullerene Small-Molecule Solar Cells, *J. Mater. Chem. A*, 2014, **2**, 1869–1876.

54 K. Vandewal, A. Gadisa, W. D. Oosterbaan, S. Bertho, F. Banishoeib, I. V. Severen, L. Lutsen, T. J. Cleij, D. Vanderzande and J. V. Manca, The Relation Between Open-Circuit Voltage and the Onset of Photocurrent Generation by Charge-Transfer Absorption in Polymer:Fullerene Bulk Heterojunction Solar Cells, *Adv. Funct. Mater.*, 2008, **18**, 2064–2070.

55 S. Gelinas, A. Rao, A. Kumar, S. L. Smith, A. W. Chin, J. Clark, T. S. van der Poll, G. C. Bazan and R. H. Friend, Ultrafast Long-Range Charge Separation in Organic Semiconductor Photovoltaic Diodes, *Science*, 2014, **343**, 512–516.

56 V. D. Mihailetchi, L. J. A. Koster, P. W. M. Blom, C. Melzer, B. de Boer, J. K. J. van Duren and R. A. J. Janssen, Compositional Dependence of the Performance of Poly(*p*-phenylene vinylene):Methanofullerene Bulk-Heterojunction Solar Cells, *Adv. Funct. Mater.*, 2005, **15**, 795–801.

57 S. R. Cowan, R. A. Street, S. Cho and A. J. Heeger, Transient Photoconductivity in Polymer Bulk Heterojunction Solar Cells: Competition between Sweep-Out and Recombination, *Phys. Rev. B: Condens. Matter Mater. Phys.*, 2011, **83**, 035205.

58 A. Sharenko, D. Gehrig, F. Laquai and T.-Q. Nguyen, The Effect of Solvent Additive on the Charge Generation and Photovoltaic Performance of a Solution-Processed Small Molecule:Perylene Diimide Bulk Heterojunction Solar Cell, *Chem. Mater.*, 2014, **26**, 4109–4118.

59 I. Riedel, J. Parisi, V. Dyakonov, L. Lutsen, D. Vanderzande and J. C. Hummelen, Effect of Temperature and Illumination on the Electrical Characteristics of Polymer–Fullerene Bulk-Heterojunction Solar Cells, *Adv. Funct. Mater.*, 2004, **14**, 38–44.

60 C. Shuttle, B. O'Regan, A. Ballantyne, J. Nelson, D. Bradley and J. Durrant, *Phys. Rev. B: Condens. Matter Mater. Phys.*, 2008, **78**, 113201.

61 K. Vandewal, K. Tvingstedt, A. Gadisa, O. Inganäs and J. V. Manca, On the origin of the open-circuit voltage of polymer–fullerene solar cells, *Nat. Mater.*, 2009, **8**, 904–909.

62 M. D. Perez, C. Borek, S. R. Forrest and M. E. Thompson, Molecular and Morphological Influences on the Open Circuit Voltages of Organic Photovoltaic Devices, *J. Am. Chem. Soc.*, 2009, **131**, 9281–9286.

63 Z. He, B. Xiao, F. Liu, H. Wu, Y. Yang, S. Xiao, C. Wang, T. P. Russell and Y. Cao, Single-junction polymer solar cells with high efficiency and photovoltage, *Nat. Photonics*, 2015, **9**, 174–179.

64 T. Heumueller, T. M. Burke, W. R. Mateker, I. T. Sachs-Quintana, K. Vandewal, C. J. Brabec and M. D. McGehee, Disorder-Induced Open-Circuit Voltage Losses in Organic Solar Cells During Photoinduced Burn-In, *Adv. Energy Mater.*, 2015, 1500111.

65 T. Schiros, G. Kladnik, D. Prezzi, A. Ferretti, G. Olivieri, A. Cossaro, L. Floreano, A. Verdini, C. Schenck, M. Cox, A. A. Gorodetsky, K. Plunkett, D. Delongchamp, C. Nuckolls, A. Morgante, D. Cvetko and I. Kymissis,

Published on 08 2015. Downloaded on 06/08/2025 2:35:09 .

Donor–Acceptor Shape Matching Drives Performance in Photovoltaics, *Adv. Energy Mater.*, 2013, **3**, 894.

66 K. R. Graham, C. Cabanetos, J. P. Jahnke, M. N. Idso, A. El Labban, G. O. Ngongang Ndjawa, T. Heumueller, K. Vandewal, A. Salleo, B. F. Chmelka, A. Amassian, P. M. Beaujuge and M. D. McGehee, Importance of the Donor: Fullerene Intermolecular Arrangement for High-Efficiency Organic Photovoltaics, *J. Am. Chem. Soc.*, 2014, **136**, 9608–9618.

67 T. W. Holcombe, J. E. Norton, J. Rivnay, C. H. Woo, L. Goris, C. Piliego, G. Griffini, A. Sellinger, J. L. Bredas, A. Salleo and J. M. Frechet, Steric Control of the Donor/Acceptor Interface: Implications in Organic Photovoltaic Charge Generation, *J. Am. Chem. Soc.*, 2011, **133**, 12106–12114.

68 A. L. Tang, C. L. Zhan and J. N. Yao, Comparative Study of Effects of Terminal Non-Alkyl Aromatic and Alkyl Groups on Small-Molecule Solar Cell Performance, *Adv. Energy Mater.*, 2015, **5**, 1500059.

69 Y. Zhao, Y. Guo and Y. Liu, 25th Anniversary Article: Recent Advances in n-Type and Ambipolar Organic Field-Effect Transistors, *Adv. Mater.*, 2013, **25**, 5372–5391.

70 F. Würthner, Perylene bisimide dyes as versatile building blocks for functional supramolecular architectures, *Chem. Commun.*, 2004, 1564–1579.

71 D. M. Ke, C. L. Zhan, S. P. Xu, X. L. Ding, A. D. Peng, J. Sun, S. G. He, A. D. Q. Li and J. N. Yao, Self-Assembled Hollow Nanospheres Strongly Enhance Photoluminescence, *J. Am. Chem. Soc.*, 2011, **133**, 11022–11025.

72 Z. G. Zhang, C. L. Zhang, X. Zhang, S. L. Zhang, J. H. Huang, A. D. Q. Li and J. N. Yao, A Self-Assembling Phase Diagram from Amphiphilic Perylene Diimides, *Chem.–Eur. J.*, 2012, **18**, 12305–12313.

73 J. J. Dittmer, E. A. Marseglia and R. H. Friend, Electron Trapping in Dye/Polymer Blend Photovoltaic Cells, *Adv. Mater.*, 2000, **12**, 1270–1274.

74 A. Sharenko, C. M. Proctor, T. S. van der Poll, Z. B. Henson, T.-Q. Nguyen and G. C. Bazan, A High-Performing Solution-Processed Small Molecule:Perylene Diimide Bulk Heterojunction Solar Cell, *Adv. Mater.*, 2013, **25**, 4403–4407.

75 Y. X. Chen, X. Zhang, C. L. Zhan and J. N. Yao, In-Depth Understanding of Photocurrent Enhancement in Solution-Processed Small-Molecule:Perylene-Diimide Non-fullerene Organic Solar Cells, *Phys. Status Solidi A*, 2015, **212**, 1961–1968.

76 L. J. Huo, S. Q. Zhang, X. Guo, F. Xu, Y. F. Li and J. H. Hou, Replacing Alkoxy Groups with Alkylthienyl Groups: A Feasible Approach To Improve the Properties of Photovoltaic Polymers, *Angew. Chem., Int. Ed.*, 2011, **50**, 9697–9702.

77 R. Singh, E. Aluicio-Sarduy, Z. Kan, T. Ye, R. C. I. MacKenzie and P. E. Keivanidis, Fullerene-free organic solar cells with an efficiency of 3.7% based on a low-cost geometrically planar perylene diimide monomer, *J. Mater. Chem. A*, 2014, **2**, 14348–14353.

78 T. Ye, R. Singh, H.-J. Butt, G. Floudas and P. E. Keivanidis, Effect of Local and Global Structural Order on the Performance of Perylene Diimide Excimeric Solar Cells, *ACS Appl. Mater. Interfaces*, 2013, **5**, 11844–11857.

79 E. Aluicio-Sarduy, R. Singh, Z. Kan, T. Ye, A. Baidak, A. Calloni, G. Berti, L. Duò, A. Iosifidis, S. Beaupré, M. Leclerc, H.-J. Butt, G. Floudas and P. E. Keivanidis, Elucidating the Impact of Molecular Packing and Device Architecture on the Performance of Nanostructured Perylene Diimide Solar Cells, *ACS Appl. Mater. Interfaces*, 2015, **7**, 8687–8698.

80 D. W. Gehrig, S. Roland, I. A. Howard, V. Kamm, H. Mangold, D. Neher and F. Laquai, Efficiency-Limiting Processes in Low-Bandgap Polymer: Perylene Diimide Photovoltaic Blends, *J. Phys. Chem. C*, 2014, **118**, 20077–20085.

81 S. Shoaee, F. Deledalle, P. S. Tuladhar, R. Shivanna, S. Rajaram, K. S. Narayan and J. R. Durrant, A Comparison of Charge Separation Dynamics in Organic Blend Films Employing Fullerene and Perylene Diimide Electron Acceptors, *J. Phys. Chem. Lett.*, 2015, **6**, 201–205.

82 X. L. Zhang, B. Jiang, X. Zhang, J. H. Huang, C. L. Zhan and J. N. Yao, Cooperatively Tuning Phase Size and Absorption of Near IR Photons in P3HT: Perylene Diimide Solar Cells by Bay-Modifications on the Acceptor, *J. Phys. Chem. C*, 2014, **118**, 24212–24220.

83 Y. Cai, L. Huo, X. Sun, D. Wei, M. Tang and Y. Sun, High Performance Organic Solar Cells Based on a Twisted Bay-Substituted Tetraphenyl Functionalized Perylenediimide Electron Acceptor, *Adv. Energy Mater.*, 2015, 1500032.

84 P. E. Hartnett, A. Timalsina, H. S. S. R. Matte, N. Zhou, X. Guo, W. Zhao, A. Facchetti, R. P. H. Chang, M. C. Hersam, M. R. Wasielewski and T. J. Marks, Slip-Stacked Perylenediimides as an Alternative Strategy for High Efficiency Nonfullerene Acceptors in Organic Photovoltaics, *J. Am. Chem. Soc.*, 2014, **136**, 16345–16356.

85 S. Rajaram, R. Shivanna, S. K. Kandappa and K. S. Narayan, Nonplanar Perylene Diimides as Potential Alternatives to Fullerenes in Organic Solar Cells, *J. Phys. Chem. Lett.*, 2012, **3**, 2405–2408.

86 L. Ye, K. Sun, W. Jiang, S. Zhang, W. Zhao, H. Yao, Z. Wang and J. Hou, Enhanced Efficiency in Fullerene-Free Polymer Solar Cell by Incorporating Fine-designed Donor and Acceptor Materials, *ACS Appl. Mater. Interfaces*, 2015, **7**(17), 9274–9280.

87 C.-H. Wu, C.-C. Chueh, Y.-Y. Xi, H.-L. Zhong, G.-P. Gao, Z.-H. Wang, L. D. Pozzo, T.-C. Wen and A. K.-Y. Jen, Influence of Molecular Geometry of Perylene Diimide Dimers and Polymers on Bulk Heterojunction Morphology Toward High-Performance Nonfullerene Polymer Solar Cells, *Adv. Funct. Mater.*, 2015, **25**, 5326–5332.

88 X. Zhang, J. N. Yao and C. L. Zhan, Synthesis and Photovoltaic Properties of Low Bandgap Dimeric Perylene Diimide Based Non-Fullerene Acceptors, *Sci. China: Chem.*, 2015, DOI: SCC-2015-0241.

89 X. Zhang, J. N. Yao and C. L. Zhan, Selenophenyl Bridged Perylene Diimide Dimer as Efficient Solution-Processable Small Molecule Acceptor, *Chem. Commun.*, 2015, **51**, 1058–1061.

 This journal is © The Royal Society of Chemistry 2015

Published on 08 2015. Downloaded on 06/08/2025 2:35:09 .

90 Y. X. Chen, X. Zhang, C. L. Zhang and J. N. Yao, Origin of Effects of Additive Solvent on Film-Morphology in Solution-ProcessedNon-Fullerene Solar Cells, *ACS Appl. Mater. Interfaces*, 2015, **7**, 6462–6471.
91 X. Zhang, C. L. Zhan and J. N. Yao, Non-Fullerene Organic Solar Cells with 6.1% Efficiency through Fine-Tuning Parameters of Film-Forming Process, *Chem. Mater.*, 2015, **27**, 166–173.
92 Z. H. Lu, B. Jiang, X. Zhang, A. L. Tang, L. L. Chen, C. L. Zhan and J. N. Yao, Perylene-Diimide Based Non-Fullerene Solar Cells with 4.34% Efficiency through Engineering Surface D/A Compositions, *Chem. Mater.*, 2014, **26**, 2907–2914.
93 Y. Lin, J. Wang, S. Dai, Y. Li, D. Zhu and X. Zhan, A Twisted Dimeric Perylene Diimide Electron Acceptor for Efficient Organic Solar Cells, *Adv. Energy Mater.*, 2014, **4**, 1400420.
94 J. Wang, Y. Yao, S. Dai, X. Zhang, W. Wang, Q. He, L. Han, Y. Lin and X. Zhan, Oligothiophene-bridged perylene diimide dimers for fullerene-free polymer solar cells: effect of bridge length, *J. Mater. Chem. A*, 2015, **3**, 13000–13010.
95 J. Zhao, Y. Li, H. Lin, Y. Liu, K. Jiang, C. Mu, T. Ma, J. Y. L. Lai, H. Hu, D. Yu and H. Yan, High-efficiency non-fullerene organic solar cells enabled by a difluorobenzothiadiazole-based donor polymer combined with a properly matched small molecule acceptor, *Energy Environ. Sci.*, 2015, **8**, 520–525.
96 W. Jiang, L. Ye, X. Li, X. Ciao, F. Tan, W. Zhao, J. Hou and Z. Wang, Bay-linked Perylene Bisimides as Promising Non-Fullerene Acceptors for Organic Solar Cells, *Chem. Commun.*, 2014, **50**, 1024–1026.
97 L. Ye, W. Jiang, W. Zhao, S. Zhang, D. Qian, Z. Wang and J. Hou, Selecting a Donor Polymer for Realizing Favorable Morphology in Efficient Non-fullerene Acceptor-based Solar Cells, *Small*, 2014, **10**, 4658–4663.
98 L. Ye, W. Jiang, W. Zhao, S. Zhang, Y. Cui, Z. Wang and J. Hou, Toward efficient non-fullerene polymer solar cells: Selection of donor polymers, *Org. Electron.*, 2015, **17**, 295–303.
99 Y. Fu, Q. Yang, Y. Deng, W. Jiang, Z. Wang, Y. Geng and Z. Xie, Suppressed charge recombination in polymer solar cells based on perylene diimide derivative acceptors *via* solvent vapor annealing, *Org. Electron.*, 2015, **18**, 24–31.
100 Y. Zang, C.-Z. Li, C.-C. Chueh, S. T. Williams, W. Jiang, Z.-H. Wang, J.-S. Yu and A. K.-Y. Jen, Integrated Molecular, Interfacial, and Device Engineering towards High-Performance Non-Fullerene Based Organic Solar Cells, *Adv. Mater.*, 2014, **26**, 5708–5714.
101 D. Sun, D. Meng, Y. Cai, B. Fan, Y. Li, W. Jiang, L. Huo, Y. Sun and Z. Wang, Non-Fullerene-Acceptor-Based Bulk-Heterojunction Organic Solar Cells with Efficiency over 7%, *J. Am. Chem. Soc.*, 2015, **137**, 11156–11162.
102 Y. Zhong, M. T. Trinh, R. Chen, W. Wang, P. P. Khlyabich, B. Kumar, Q. Xu, C.-Y. Nam, M. Y. Sfeir, C. Black, M. L. Steigerwald, Y.-L. Loo, S. Xiao, F. Ng, X.-Y. Zhu and C. Nuckolls, Efficient Organic Solar Cells with Helical Perylene Diimide Electron Acceptors, *J. Am. Chem. Soc.*, 2014, **136**, 15215–15221.
103 B. A. Gregg, Entropy of Charge Separation in Organic Photovoltaic Cells: The Benefit of Higher Dimensionality, *J. Phys. Chem. Lett.*, 2011, **2**, 3013–3015.
104 X. Zhang, B. Jiang, S. Zhang, J. Hou, J. N. Yao and C. L. Zhan, Solution-processible perylene diimide based star-shaped small molecule acceptor: Synthesis and photovoltaic properties, *Proc. SPIE, Organic Photovoltaics XV*, 2014, vol. 9184, p. 91840C.
105 Y. Lin, Y. Wang, J. Wang, J. Hou, Y. Li, D. Zhu and X. Zhan, A Star-Shaped Perylene Diimide Electron Acceptor for High-Performance Organic Solar Cells, *Adv. Mater.*, 2014, **26**, 5137–5142.
106 Y. Liu, C. Mu, K. Jiang, J. Zhao, Y. Li, L. Zhang, Z. Li, J. Y. L. Lai, H. Hu, T. Ma, R. Hu, D. Yu, X. Huang, B. Z. Tang and H. Yan, A Tetraphenylethylene Core-Based 3D Structure Small Molecular Acceptor Enabling Efficient Non-Fullerene Organic Solar Cells, *Adv. Mater.*, 2015, **27**, 1015–1020.
107 Y. Liu, J. Y. L. Lai, S. Chen, Y. Li, K. Jiang, J. Zhao, Z. Li, H. Hu, T. Ma, H. Lin, J. Liu, J. Zhang, F. Huang, D. Yu and H. Yan, Efficient non-fullerene polymer solar cells enabled by tetrahedron-shaped core based 3D-structure small-molecular electron acceptors, *J. Mater. Chem. A*, 2015, **3**, 13632–13636.
108 W. Chen, X. Yang, G. Long, X. Wan, Y. Chen and Q. Zhang, A perylene diimide (PDI)-based small molecule with tetrahedral configuration as a non-fullerene acceptor for organic solar cells, *J. Mater. Chem. C*, 2015, **3**, 4698–4705.
109 C. B. Nielsen, E. Voroshazi, S. Holliday, K. Cnops, D. Cheyns and I. McCulloch, Electron-deficient truxenone derivatives and their use in organic photovoltaics, *J. Mater. Chem. A*, 2014, **2**, 12348–12354.
110 T. Zhou, T. Jia, B. Kang, F. Li, M. Fahlman and Y. Wang, Nitrile-Substituted QA Derivatives: New Acceptor Materials for Solution-Processable Organic Bulk Heterojunction Solar Cells, *Adv. Energy Mater.*, 2011, **1**, 431–439.
111 Y. Zhou, L. Ding, K. Shi, Y.-Z. Dai, N. Ai, J. Wang and J. Pei, A Non-Fullerene Small Molecule as Efficient Electron Acceptor in Organic Bulk Heterojunction Solar Cells, *Adv. Mater.*, 2012, **24**, 957–961.
112 Y. Zhou, Y.-Z. Dai, Y.-Q. Zheng, X.-Y. Wang, J.-Y. Wang and J. Pei, Non-fullerene acceptors containing fluoranthene-fused imides for solution-processed inverted organic solar cells, *Chem. Commun.*, 2013, **49**, 5802–5804.
113 H. Li, T. Earmme, S. Subramaniyan and S. A. Jenekhe, Bis(Naphthalene Imide)diphenylanthrazolines: A New Class of Electron Acceptors for Efficient Nonfullerene Organic Solar Cells and Applicable to Multiple Donor Polymers, *Adv. Energy Mater.*, 2015, 1402041.
114 H. Li, T. Earmme, G. Ren, A. Saeki, S. Yoshikawa, N. M. Murari, S. Subramaniyan, M. J. Crane, S. Seki and S. A. Jenekhe, Beyond Fullerenes: Design of Nonfullerene Acceptors for Efficient Organic Photovoltaics, *J. Am. Chem. Soc.*, 2014, **136**, 14589–14597.

Published on 08 2015. Downloaded on 06/08/2025 2:35:09 .

115 H. Li, Y.-J. Hwang, B. A. E. Courtright, F. N. Eberle, S. Subramaniyan and S. A. Jenekhe, Fine-Tuning the 3D Structure of Nonfullerene Electron Acceptors Toward High-Performance Polymer Solar Cells, *Adv. Mater.*, 2015, **27**, 3266–3272.

116 C.-P. Chen, S.-H. Chan, T.-C. Chao, C. Ting and B.-T. Ko, Low-Bandgap Poly(Thiophene-Phenylene-Thiophene) Derivatives with Broaden Absorption Spectra for Use in High-Performance Bulk-Heterojunction Polymer Solar Cells, *J. Am. Chem. Soc.*, 2008, **130**, 12828–12833.

117 Y.-X. Xu, C.-C. Chueh, H.-L. Yip, F.-Z. Ding, Y.-X. Li, C.-Z. Li, X. Li, W.-C. Chen and A. K. Y. Jen, Improved Charge Transport and Absorption Coefficient in Indacenodithieno[3,2-*b*]thiophene-based Ladder-Type Polymer Leading to Highly Efficient Polymer Solar Cells, *Adv. Mater.*, 2012, **24**, 6356–6361.

118 Z.-G. Zhang, B. Qi, Z. Jin, D. Chi, Z. Qi, Y. Li and J. Wang, Perylene diimides: a thickness-insensitive cathode interlayer for high performance polymer solar cells, *Energy Environ. Sci.*, 2014, **7**, 1966–1973.

119 Y. Lin, Z.-G. Zhang, H. Bai, J. Wang, Y. Yao, Y. Li, D. Zhu and X. Zhan, High-performance fullerene-free polymer solar cells with 6.31% efficiency, *Energy Environ. Sci.*, 2015, **8**, 610–616.

120 Y. Lin, J. Wang, Z.-G. Zhang, H. Bai, Y. Li, D. Zhu and X. Zhan, An Electron Acceptor Challenging Fullerenes for Efficient Polymer Solar Cells, *Adv. Mater.*, 2015, **27**, 1170–1174.

121 T. V. Pho, F. M. Toma, M. L. Chabinyc and F. Wudl, Self-Assembling Decacyclene Triimides Prepared through a Regioselective Hextuple Friedel–Crafts Carbamylation, *Angew. Chem., Int. Ed.*, 2013, **52**, 1446–1451.

122 Z. Mao, W. Senevirathna, J.-Y. Liao, J. Gu, S. V. Kesava, C. Guo, E. D. Gomez and G. Sauvé, Azadipyrromethene-Based Zn(II) Complexes as Nonplanar Conjugated Electron Acceptors for Organic Photovoltaics, *Adv. Mater.*, 2014, **26**, 6290–6294.

123 F. G. Brunetti, X. Gong, M. Tong, A. J. Heeger and F. Wudl, Strain and Hückel Aromaticity: Driving Forces for a Promising New Generation of Electron Acceptors in Organic Electronics, *Angew. Chem., Int. Ed.*, 2010, **49**, 532–536.

124 Z. Mao, T. P. Le, K. Vakhshouri, R. Fernando, F. Ruan, E. Muller, E. D. Gomez and G. Sauvé, Processing additive suppresses phase separation in the active layer of organic photovoltaics based on naphthalene diimide, *Org. Electron.*, 2014, **15**, 3384–3391.

125 E. Ahmed, G. Ren, F. S. Kim, E. C. Hollenbeck and S. A. Jenekhe, Design of New Electron Acceptor Materials for Organic Photovoltaics: Synthesis, Electron Transport, Photophysics, and Photovoltaic Properties of Oligothiophene-Functionalized Naphthalene Diimides, *Chem. Mater.*, 2011, **23**, 4563–4577.

126 X. Wang, J. H. Huang, Z. X. Niu, Y. X. Sun and C. L. Zhan, Dimeric Naphthalene Diimide Based Small Molecule Acceptors: Synthesis, Characterization, and Photovoltaic Properties, *Tetrahedron*, 2014, **70**, 4726–4731.

127 Y. Liu, L. Zhang, H. Lee, H.-W. Wang, A. Santala, F. Liu, Y. Diao, A. L. Briseno and T. P. Russell, NDI-Based Small Molecule as Promising Nonfullerene Acceptor for Solution-Processed Organic Photovoltaics, *Adv. Energy Mater.*, 2015, 1500195.

128 C. H. Woo, T. W. Holcombe, D. A. Unruh, A. Sellinger and J. M. J. Fréchet, Phenyl *vs.* Alkyl Polythiophene: A Solar Cell Comparison Using a Vinazene Derivative as Acceptor, *Chem. Mater.*, 2010, **22**, 1673–1679.

129 B. Walker, X. Han, C. Kim, A. Sellinger and T.-Q. Nguyen, Solution-Processed Organic Solar Cells from Dye Molecules: An Investigation of Diketopyrrolopyrrole:Vinazene Heterojunctions, *ACS Appl. Mater. Interfaces*, 2012, **4**, 244–250.

130 J. T. Bloking, X. Han, A. T. Higgs, J. P. Kastrop, L. Pandey, J. E. Norton, C. Risko, C. E. Chen, J.-L. Brédas, M. D. McGehee and A. Sellinger, Solution-Processed Organic Solar Cells with Power Conversion Efficiencies of 2.5% using Benzothiadiazole/Imide-Based Acceptors, *Chem. Mater.*, 2011, **23**, 5484–5490.

131 J. T. Bloking, T. Giovenzana, A. T. Higgs, A. J. Ponec, E. T. Hoke, K. Vandewal, S. Ko, Z. Bao, A. Sellinger and M. D. McGehee, Comparing the Device Physics and Morphology of Polymer Solar Cells Employing Fullerenes and Non-Fullerene Acceptors, *Adv. Energy Mater.*, 2014, **4**, 1301426.

132 J. D. Douglas, M. S. Chen, J. R. Niskala, O. P. Lee, A. T. Yiu, E. P. Young and J. M. J. Fréchet, Solution-Processed, Molecular Photovoltaics that Exploit Hole Transfer from Non-Fullerene, n-Type Materials, *Adv. Mater.*, 2014, **26**, 4313–4319.

133 K. N. Winzenberg, P. Kemppinen, F. H. Scholes, G. E. Collis, Y. Shu, T. B. Singh, A. Bilic, C. M. Forsyth and S. E. Watkins, Indan-1,3-dione electron-acceptor small molecules for solution-processable solar cells: a structure–property correlation, *Chem. Commun.*, 2013, **49**, 6307–6309.

134 Y. Kim, C. E. Song, S.-J. Moonc and E. Lim, Rhodanine dye-based small molecule acceptors for organic photovoltaic cells, *Chem. Commun.*, 2014, **50**, 8235–8238.

135 S. Holliday, R. S. Ashraf, C. B. Nielsen, M. Kirkus, J. A. Röhr, C.-H. Tan, E. Collado-Fregoso, A.-C. Knall, J. R. Durrant, J. Nelson and I. McCulloch, A Rhodanine Flanked Nonfullerene Acceptor for Solution-Processed Organic Photovoltaics, *J. Am. Chem. Soc.*, 2015, **137**, 898–904.

136 O. K. Kwon, J.-H. Park, S. K. Park and S. Y. Park, Soluble Dicyanodistyrylbenzene-Based Non-Fullerene Electron Acceptors with Optimized Aggregation Behavior for High-Efficiency Organic Solar Cells, *Adv. Energy Mater.*, 2014, 1400929.

137 O. K. Kwon, J.-H. Park, D. W. Kim, S. K. Park and S. Y. Park, An All-Small-Molecule Organic Solar Cell with High Efficiency Nonfullerene Acceptor, *Adv. Mater.*, 2015, **27**, 1951–1956.

138 R.-Q. Lu, Y.-Q. G. Zheng, Y.-N. Zhou, X.-Y. Yan, T. Lei, K. Shi, Y. Zhou, J. Pei, L. Zoppi, K. K. Baldridge, J. S. Siegeld and X.-Y. Cao, Corannulene derivatives as

 This journal is © The Royal Society of Chemistry 2015

Published on 08 2015. Downloaded on 06/08/2025 2:35:09 .

non-fullerene acceptors in solution-processed bulk heterojunction solar cells, *J. Mater. Chem. A*, 2014, **2**, 20515–20519.

139 C. G. Claessens, D. González-Rodríguez and T. Torres, Subphthalocyanines: Singular Nonplanar Aromatic CompoundssSynthesis, Reactivity, and Physical Properties, *Chem. Rev.*, 2002, **102**, 835–853.

140 B. Verreet, B. P. Rand, D. Cheyns, A. Hadipour, T. Aernouts, P. Heremans, A. Medina, C. G. Claessens and T. Torres, A 4% Efficient Organic Solar Cell Using a Fluorinated Fused Subphthalocyanine Dimer as an Electron Acceptor, *Adv. Energy Mater.*, 2011, **1**, 565–568.

141 G. E. Morse, J. L. Gantz, K. X. Steirer, N. R. Armstrong and T. P. Bender, Pentafluorophenoxy Boron Subphthalocyanine (F5BsubPc) as a Multifunctional Material for Organic Photovoltaics, *ACS Appl. Mater. Interfaces*, 2014, **6**, 1515–1524.

142 B. Verreet, K. Cnops, D. Cheyns, P. Heremans, A. Stesmans, G. Zango, C. G. Claessens, T. Torres and B. P. Rand, Decreased Recombination Through the Use of a Non-Fullerene Acceptor in a 6.4% Efficient Organic Planar Heterojunction Solar Cell, *Adv. Energy Mater.*, 2014, **4**, 1301413.

143 K. Cnops, B. P. Rand, D. Cheyns, B. Verreet, M. A. Empl and P. Heremans, 8.4% efficient fullerene-free organic solar cells exploiting long-range exciton energy transfer, *Nat. Commun.*, 2014, **5**, 3406.

144 P. Sullivan, G. E. Collis, L. A. Rochford, J. F. Arantes, P. Kemppinen, T. S. Jones and K. N. Winzenberg, An *N*-ethylated barbituric acid end-capped bithiophene as an electron-acceptor material in fullerene-free organic photovoltaics, *Chem. Commun.*, 2015, **51**, 6222–6225.

145 A. N. Bartynski, M. Gruber, S. Das, S. Rangan, S. Mollinger, C. Trinh, S. E. Bradforth, K. Vandewal, A. Salleo, R. A. Bartynski, W. Bruetting and M. E. Thompson, Symmetry-Breaking Charge Transfer in a Zinc Chlorodipyrrin Acceptor for High Open Circuit Voltage Organic Photovoltaics, *J. Am. Chem. Soc.*, 2015, **137**, 5397–5405.

146 C. B. Nielsen, E. Voroshazi, S. Holliday, K. Cnops, D. Cheyns and I. McCulloch, Electron-deficient truxenone derivatives and their use in organic photovoltaics, *J. Mater. Chem. A*, 2014, **2**, 12348–12354.

147 Y. Zhou, T. Kurosawa, W. Ma, Y. Guo, L. Fang, K. Vandewal, Y. Diao, C. Wang, Q. Yan, J. Reinspach, J. Mei, A. L. Appleton, G. I. Koleilat, Y. Gao, S. C. B. Mannsfeld, A. Salleo, H. Ade, D. Zhao and Z. Bao, High Performance All-Polymer Solar Cell *via* Polymer Side-Chain Engineering, *Adv. Mater.*, 2014, **26**, 3767–3772.

148 Y. Zhou, Q. Yan, Y.-Q. Zheng, J.-Y. Wang, D. Zhao and J. Pei, New polymer acceptors for organic solar cells: the effect of regio-regularity and device configuration, *J. Mater. Chem. A*, 2013, **1**, 6609–6613.

149 P. Cheng, L. Ye, X. Zhao, J. Hou, Y. Li and X. Zhan, Binary additives synergistically boost the efficiency of all-polymer solar cells up to 3.45%, *Energy Environ. Sci.*, 2014, **7**, 1351–1356.

150 J. Cao, Q. Liao, X. Du, J. Chen, Z. Xiao, Q. Zuo and L. Ding, A pentacyclic aromatic lactam building block for efficient polymer solar cells, *Energy Environ. Sci.*, 2013, **6**, 3224–3228.

151 I. H. Jung, W.-Y. Lo, J. Jang, W. Chen, D. Zhao, E. S. Landry, L. Lu, D. V. Talapin and L. Yu, Synthesis and Search for Design Principles of New Electron Accepting Polymers for All-Polymer Solar Cells, *Chem. Mater.*, 2014, **26**, 3450–3459.

152 I. H. Jung, D. Zhao, J. Jang, W. Chen, E. S. Landry, L. Lu, D. V. Talapin and L. Yu, Development and Structure/Property Relationship of New Electron Accepting Polymers Based on Thieno[2′,3′:4,5]pyrido[2,3-*g*]thieno[3,2-*c*]quinoline-4,10-dione for All-Polymer Solar Cells, *Chem. Mater.*, 2015, **27**, 5941–5948.

153 W. Zhou, Z.-G. Zhang, L. Ma, Y. Li and X. Zhan, Dithienocoronenediimidebasedconjugatedpolymersaselectron acceptors for all-polymersolarcells, *Sol. Energy Mater. Sol. Cells*, 2013, **112**, 13–19.

154 Y. Jiang, L. Lu, M. Yang, C. Zhan, Z. Xie, F. Verpoorta and S. Xiao, Taking the place of perylene diimide: perylene tetracarboxylic tetraester as a building block for polymeric acceptors to achieve higher open circuit voltage in all-polymer bulk heterojunction solar cells, *Polym. Chem.*, 2013, **4**, 5612–5620.

155 C. Lee, H. Kang, W. Lee, T. Kim, K.-H. Kim, H. Y. Woo, C. Wang and B. J. Kim, High-Performance All-Polymer Solar Cells Via Side-Chain Engineering of the Polymer Acceptor: The Importance of the Polymer Packing Structure and the Nanoscale Blend Morphology, *Adv. Mater.*, 2015, **27**, 2466–2471.

156 H. Kang, M. A. Uddin, C. Lee, K.-H. Kim, T. L. Nguyen, W. Lee, Y. Li, C. Wang, H. Y. Woo and B. J. Kim, Determining the Role of Polymer Molecular Weight for High-Performance All-Polymer Solar Cells: Its Effect on Polymer Aggregation and Phase Separation, *J. Am. Chem. Soc.*, 2015, **137**, 2359–2365.

157 T. Earmme, Y.-J. Hwang, N. M. Murari, S. Subramaniyan and S. A. Jenekhe, All-Polymer Solar Cells with 3.3% Efficiency Based on Naphthalene Diimide-Selenophene Copolymer Acceptor, *J. Am. Chem. Soc.*, 2013, **135**, 14960–14963.

158 Y. Kim, D. S. Chung and C. E. Park, Highly thermallystablenon-fullereneorganic solar cells:p-DTS(FBTTh2)2:P(NDI2OD-T2) bulk heterojunction, *Nano Energy*, 2015, **15**, 343–352.

159 Z. Li, J. D. A. Lin, H. Phan, A. Sharenko, C. M. Proctor, P. Zalar, Z. Chen, A. Facchetti and T.-Q. Nguyen, Competitive Absorption and In efficient Exciton Harvesting: Lessons Learned from Bulk Heterojunction Organic Photovoltaics Utilizing the Polymer Acceptor P(NDI2OD-T2), *Adv. Funct. Mater.*, 2014, **24**, 6989–6998.

160 Z. Tang, B. Liu, A. Melianas, J. Bergqvist, W. Tress, Q. Bao, D. Qian, O. Inganäs and F. Zhang, A New Fullerene-Free Bulk-Heterojunction System for Efficient High-Voltage and High-Fill Factor Solution-Processed Organic Photovoltaics, *Adv. Mater.*, 2015, **27**, 1900–1907.

161 J. W. Jung, T. P. Russell and W. H. Jo, A Small Molecule Composed of Dithienopyran and Diketopyrrolopyrrole as

Published on 08 2015. Downloaded on 06/08/2025 2:35:09 .

Versatile Electron Donor Compatible with Both Fullerene and Nonfullerene Electron Acceptors for High Performance Organic Solar Cells, *Chem. Mater.*, 2015, **27**, 4865–4870.

162 N. Zhou, H. Lin, S. J. Lou, X. Yu, P. Guo, E. F. Manley, S. Loser, P. Hartnett, H. Huang, M. R. Wasielewski, L. X. Chen, R. P. H. Chang, A. Facchetti and T. J. Marks, Morphology-Performance Relationships in High-Efficiency All-Polymer Solar Cells, *Adv. Energy Mater.*, 2014, **4**, 1300785.

163 D. Mori, H. Benten, I. Okada, H. Ohkita and S. Ito, Low-Bandgap Donor/Acceptor Polymer Blend Solar Cells with Efficiency Exceeding 4%, *Adv. Energy Mater.*, 2014, **4**, 1301006.

164 K. D. Deshmukh, T. Qin, J. K. Gallaher, A. C. Y. Liu, E. Gann, K. O'Donnell, L. Thomsen, J. M. Hodgkiss, S. E. Watkins and C. R. McNeill, Performance, morphology and photophysics of high open-circuit voltage, low band gap allpolymer solar cells, *Energy Environ. Sci.*, 2015, **8**, 332–342.

165 C. Mu, P. Liu, W. Ma, K. Jiang, J. Zhao, K. Zhang, Z. Chen, Z. Wei, Y. Yi, J. Wang, S. Yang, F. Huang, A. Facchetti, H. Ade and H. Yan, High-Efficiency All-Polymer Solar Cells Based on a Pair of Crystalline Low-Bandgap Polymers, *Adv. Mater.*, 2014, **26**, 7224–7230.

166 D. Mori, H. Benten, I. Okada, H. Ohkita and S. Ito, Highly Efficient Charge-Carrier Generation and Collection in Polymer/Polymer Blend Solar Cells with a Power Conversion Efficiency of 5.7%, *Energy Environ. Sci.*, 2014, **7**, 2939–2943.

167 J. W. Jung, J. W. Jo, C.-C. Chueh, F. Liu, W. H. Jo, T. P. Russell and A. K.-Y. Jen, Fluoro-Substituted n-Type Conjugated Polymers for Additive-Free All-Polymer Bulk Heterojunction Solar Cells with High Power Conversion Efficiency of 6.71%, *Adv. Mater.*, 2015, **27**, 3310–3317.

168 J. Choi, K.-H. Kim, H. Yu, C. Lee, H. Kang, I. Song, Y. Kim, J. H. Oh and B. J. Kim, Importance of Electron Transport Ability in Naphthalene Diimide-Based Polymer Acceptors for High-Performance, Additive-Free, All-Polymer Solar Cells, *Chem. Mater.*, 2015, **27**, 5230–5237.

169 E. Zhou, J. Cong, K. Hashimoto and K. Tajima, Control of Miscibility and Aggregation Via the Material Design and Coating Process for High-Performance Polymer Blend Solar Cells, *Adv. Mater.*, 2013, **25**, 6991–6996.

170 S. Subramaniyan, T. Earmme, N. M. Murari and S. A. Jenekhe, Naphthobisthiazole diimide-based n-type polymer semiconductors: synthesis, p-stacking, field-effect charge transport, and all-polymer solar cells, *Polym. Chem.*, 2014, **5**, 5707–5715.

171 Y.-J. Hwang, T. Earmme, S. Subramaniyan and S. A. Jenekhe, Side chain engineering of n-type conjugated polymer enhances photocurrent and efficiency of all-polymer solar cells, *Chem. Commun.*, 2014, **50**, 10801–10804.

172 Y.-J. Hwang, T. Earmme, B. A. E. Courtright, F. N. Eberle and S. A. Jenekhe, nType Semiconducting Naphthalene Diimide-Perylene Diimide Copolymers: Controlling Crystallinity, Blend Morphology, and Compatibility Toward High-Performance All-Polymer Solar Cells, *J. Am. Chem. Soc.*, 2015, **137**, 4424–4434.

173 L. M. Kozycz, D. Gao, A. J. Tilley and D. S. Seferos, One Donor–Two Acceptor (D–A1)-(D–A2) Random Terpolymers Containing Perylene Diimide, Naphthalene Diimide, and Carbazole Units, *J. Polym. Sci., Part A: Polym. Chem.*, 2014, **52**, 3337–3345.

174 Y. Cao, T. Lei, J. Yuan, J.-Y. Wang and J. Pei, Dithiazolyl-benzothiadiazole-containing polymer acceptors: synthesis, characterization, and all-polymer solar cells, *Polym. Chem.*, 2013, **4**, 5228–5236.

175 W. Li, W. S. C. Roelofs, M. Turbiez, M. M. Wienk and R. A. J. Janssen, Polymer Solar Cells with Diketopyrrolopyrrole Conjugated Polymers as the Electron Donor and Electron Acceptor, *Adv. Mater.*, 2014, **26**, 3304–3309.

176 D. Bartesaghi, I. del Carmen Pérez, J. Kniepert, S. Roland, M. Turbiez, D. Neher and L. J. A. Koster, Competition between recombination and extraction of free charges determines the fill factor of organic solar cells, *Nat. Commun.*, 2015, **6**, 7083.

This journal is © The Royal Society of Chemistry 2015